11-1-2012

Characterization of color, gloss and mechanical performance of 3D printed structures

Hrushikesh Godbole

ROCHESTER INSTITUTE OF TECHNOLOGY

Characterization of Color, Gloss and Mechanical Performance of 3D Printed Structures

A Thesis

Submitted In Partial Fulfillment of the Requirements for the Degree Of

Master of Science in Industrial and Systems Engineering

Department Of Industrial and Systems Engineering

Kate Gleason College of Engineering

Hrushikesh C. Godbole

November, 2012

DEPARTMENT OF INDUSTRIAL AND SYSTEMS ENGINEERING

KATE GLEASON COLLEGE OF ENGINEERING

ROCHESTER INSTITUTE OF TECHNOLOGY

ROCHESTER, NY

CERTIFICATE OF APPROVAL

M.S. DEGREE THESIS

The M.S. Degree Thesis of Hrushikesh C. Godbole

Has Been Examined and Approved By The

Thesis Committee as Satisfactory For The

Thesis Requirements For The

Master of Science Degree

Approved by:

_____

Dr. Marcos Esterman, Thesis Advisor

_____

Dr. Denis Cormier, Committee Member

Dedication

I offer this work at the feet of my benevolent Sadguru. His blessings have alone enabled this research.

Acknowledgements

A thesis is an academic journey through the realms of knowledge unknown. I wish to convey my gratitude towards Dr. Marcos Esterman who has always been present as a guide throughout this journey. I would also like to thank him for patience in reviewing my work with an eye for detail. His advice was never limited to just academics and I will always cherish the lessons I learnt from him throughout my life.

I would also like to thank Dr. Denis Cormier for developing and nurturing my interest in rapid prototyping. Under his expert guidance, it has been a privilege to conduct research and extend the frontiers of rapid prototyping.

I would also like to acknowledge Susan Farnand from the Munsell Color Science Laboratory for her advice on topics related to color science.

Along with committee members and advisors, colleagues are the people a graduate student can always depend upon. Alvaro Rojas has been one such great colleague to work with who has proactively offered help whenever I needed it. I would also like to thank Anuj Datar, Niranjan Damle, Sundaresan Balasubramanian and Vickrant Zunjarrao for their support and advice in various matters related to the research work.

I owe much to the Industrial and Systems Engineering department which has committed people and resources to enable me perform this research.

I would also like to recognize my room-mates Gaurang Dharap, Shagan Sah and Ankit Shah for making my days as a graduate student memorable and enjoyable. Finally, I would like to convey my deepest gratitude towards my family for their unconditional love and support throughout my life.

ABSTRACT

The demand for customized products is on a rise. As such, there is a great need for methods to efficiently satisfy this need for customization. Rapid prototyping, also known as 3D printing, is a technology that enables economic production of customized low volume products and enables expedited product development cycles. Given the importance of color as a means to differentiate products generated through 3D printing processes, accurate color reproduction is essential for broad market acceptance. Color reproduction in 2D document printing is itself a complex science; achieving similar results in 3D printing will require significant research.

This research work explores the various factors that affect accurate color reproduction in rapid prototyping. More specifically, it studies the effect of process parameters and post-processing techniques on the color reproduction achieved in powder based layer deposition process with a selective binder delivery enabled by an ink-jet print head. A systematic study of a subset of these factors was conducted using a ZCorp Z510 3D printer. The process parameters that were included in the study were color, hue, coverage, layer thickness, and binder saturation. The post-processing technique focused on the use of an infiltrant, which is commonly used to increase the mechanical strength of the printed 3D structure. The response variables of interest for this study included color response, gloss and mechanical strength. A full factorial experiment was designed in order to characterize the effect. Gloss, which contributes to the visual perception, was studied as a qualitative response. Of particular interest was the effect of process parameters and the type of post processing on the tensile strength of the specimen to identify trade-offs between quality of color reproduction and the mechanical strength required for structural integrity. Analysis of the experimental data indicates that the standard process settings, on average, generate samples that have greater color lightness and lower chroma, representing an opportunity for improvement. In addition, layer thickness was found to have a significant effect on the tensile strength as well. The process of infiltration improved both the color reproduction and mechanical properties of the 3D printed samples. The choice of infiltrant did not have a significant effect on the color reproduction but had a significant effect on the tensile strength of the part.

In this research, the effect of layer thickness on color reproduction in ink jet based 3D printing has been studied for the first time. Also, adding to the body of current research, the interaction effects of the various factors have been studied. The research intends to serve as a platform to enable color scientists to collaborate with rapid prototyping experts towards achieving full selective color throughout 3D printing in the future.

CONTENTS

TABLE OF FIGURES

TABLE OF TABLES

TABLE OF EQUATIONS

1 Introduction

1.1 Motivation

Rapid Prototyping is a layer based additive manufacturing technique that was developed in the 1980's (Chua et al., 2010; Noorani & Knovel, 2006). Compared to traditional manufacturing processes, it has low tooling costs resulting in commercial advantage when manufacturing low to medium volume parts. A parametric cost analysis of rapid prototyping against injection molding has been conducted (Hopkinson & Dickens, 2001). It indicated rapid prototyping to be a viable alternative process for low to medium volume manufacture of small parts with complex geometries. Figure 1 compares the cost per part manufactured for the rapid prototyping process of stereolithography and injection molding. It is indicative of the production volumes under which rapid prototyping process are desirable.

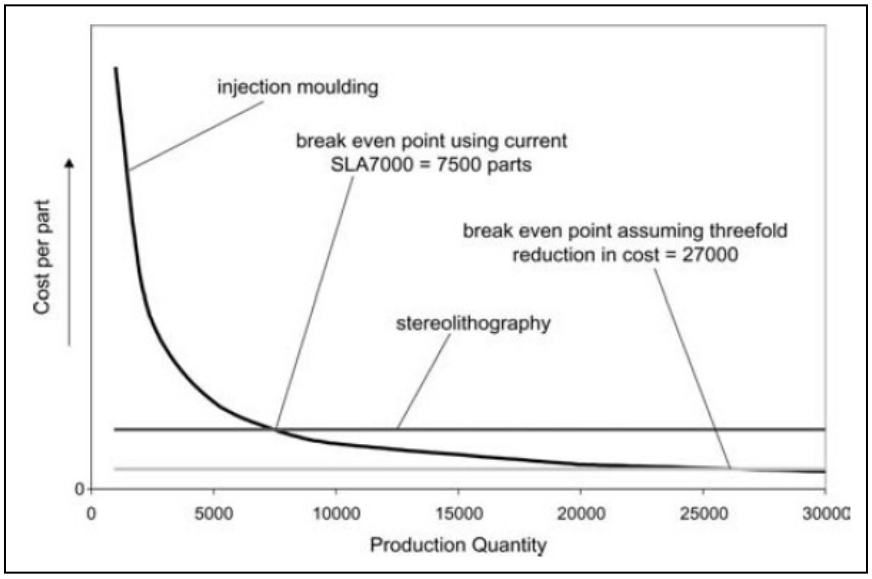

Figure 1: Comparison of variation of cost per part in stereolithography and injection molding

One of the competitive differentiators of rapid prototyping processes based on additive manufacturing is the ability to selectively color the part. The importance of color in making rapid prototyping a mature communication tool has been identified by (Rees, 1998). Color perception of an object is of great importance to human beings, as it is a vital stimulus that human beings use to sense the environment around them. The information communicated by the visual appearance of a part is greatly enhanced when the object is colored. Thus, it is of great value to incorporate color into rapid prototyping if it is to compete with colored injection molded parts, which as a process has much less flexibility to incorporate color.

The only commercially available rapid prototyping system that has incorporated selective coloring of the part is Z Corp. This system was initially developed at the Massachusetts Institute of Technology

(Sachs et al., 1993) and is capable of coloring the skin layer of the printed 3D parts. A model of the human heart printed by a Z Corp system is shown in Figure 2. It is a good example of how color greatly enhances the information conveyed as the different structures, such as veins, arteries and muscles can be clearly differentiated. However, as noted above, the current systems are only capable of coloring the surface layers. The ability to selectively color within the entire part would convey greater information, particularly for models in medical applications where the color would more clearly show anatomical features and information across cross sections (Im et al., 2002).

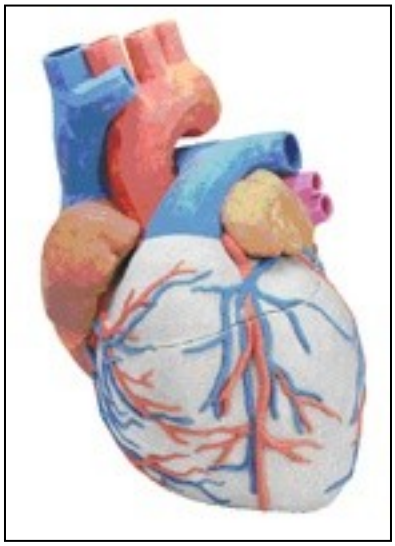

Figure 2: A 3D color model printed using Z Corp

It is also envisioned that the ability to color a part beyond its surfaces layers would help to prevent failure modes associated with the degradation of the part's aesthetics during its use. For example, it is easy to imagine surface damage due to flaking off of the skin layer due to scratches, abrasion and wear. A part that has color deeper than this surface layer would be more resistant to these failure modes.

These examples illustrate the value that can be derived from the ability to selectively color parts and the competitive advantage that this can give a rapid prototyping process relative to more conventional manufacturing processes, such as injection molding. Thus, the investigation of factors that affect the ability of multi layer deposition processes to reproduce accurate color is of great importance. The goal of the research study is to further the development of rapid prototyping as an alternative to conventional manufacturing processes, such as injection molding, by better understanding the factors that affect the color performance of these processes. In particular, the study will examine the process parameters of the Z Corp system to further our understanding of the parameters that affect the color appearance of 3D printed parts and the resulting effect on performance parameters, such as the mechanical strength of the part.

1.2 Background

This research study is multi-disciplinary in nature. In order to establish the state of the art, it is first necessary to provide background in the technologies involved, as well as in the field of color science. This chapter introduces an overview of rapid prototyping, as well as two specific techniques of rapid prototyping, namely electrophotographic rapid prototyping and inkjet based rapid prototyping. This section concludes with a discussion of the elementary principles of color science.

1.2.1 Rapid Prototyping

Rapid Prototyping is a group of fabrication processes that use additive layer manufacturing techniques. The term 3D printing and additive manufacturing are also used to describe the same rapid prototyping process. For convenience, the term rapid prototyping will be used in this document. It is a fairly recent technology compared to other conventional fabrication processes, and it emerged in the late 1980's (Chua et al., 2010; Noorani & Knovel, 2006). The process consists of the following four steps:

- Generate the geometry to be fabricated in a CAD model
- Create virtual slices of the CAD model
- Deposit a layer of material according to the geometry in that slice of the CAD model
- Successively deposit further layers till the 3D geometry is completed.

Early applications of rapid prototyping were limited to prototype exhibitions and demonstrations. However, it has since evolved, and today it is possible to manufacture functional parts of metals, plastics and ceramics using rapid prototyping (Chua et al., 2010). Rapid prototyping is best suited for the fabrication of low volume customized parts. Also, it can fabricate parts of materials like titanium that are difficult to process using conventional manufacturing techniques. Another important advantage of rapid prototyping is the ability to fabricate parts of any complexity without expensive tooling. As a result, the fixed cost associated with the manufacture of rapid prototyped parts is relatively small. Also, the lead time associated with producing prototypes is greatly reduced. From a product development stand point, this is a desirable trait as it leads to the early visualization of form and function which can led to the early detection of design errors. In today's environment of shrinking product lifecycles rapid prototyping holds a great promise to aid product development organizations to achieve competitive advantage.

Given the merits of rapid prototyping over conventional manufacturing processes, it has grown to become a very active research area over the last two decades. One of the limitations of rapid prototyping is the trade-off between part resolution and process speed. Fabrication of high resolution parts at a high process speed is a challenge with the current state of the art rapid prototyping technologies(Chua et al., 2010; Noorani & Knovel, 2006).

Being a relatively new technology much research is still needed to realize the true potential of rapid prototyping. Small breakthroughs in rapid prototyping will go a long way toward successful integration of rapid prototyping into the existing manufacturing process environment.

1.2.1.1 Electrophotography based Rapid Prototyping

Recently, there has been research interest in the development of an electrophotographic based laser printing process to print 3D objects (Jones et al., 2010). In this section, a brief discussion of electrophotography (EP) is first presented followed by a discussion on EP-based rapid prototyping.

The image reproduction processes that use light and electricity are collectively termed as electrophotography. This technique was invented by Chester Carlson in 1938. The EP printing that we find to in today's commercial laser printers was demonstrated to be feasible in 1950. Color EP printing was introduced in 1993 by QMS who introduced the ColourScript Laser 1000 color laser printer.

EP printing consists of six stages: charging, selective discharge, development, transfer, fusing and cleaning. This is illustrated in Figure 3 and the basic process of laser printing is described below.

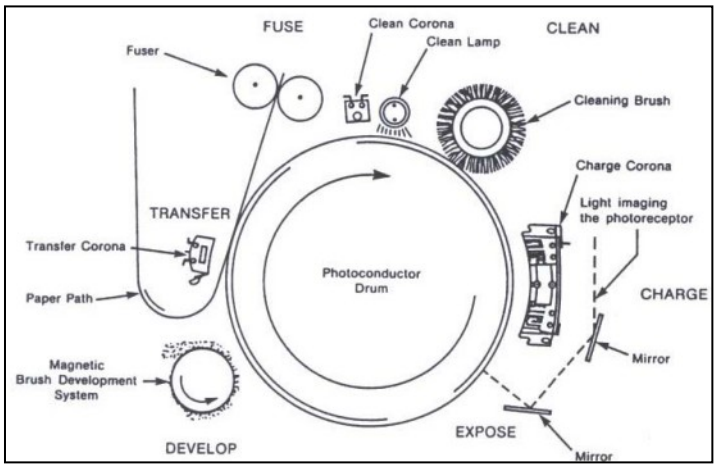

Figure 3: Work flow in electrophotography (Schein 1996)

Charging

Initially a negative charge is imparted on a photoconductive surface by either a corona wire carrying electric current or a charge roller that is in contact with the photoconductor.

Image Exposure

The photoconductor is selectively discharged by an exposure laser or LED light source. An electrostatic image area is now formed on the photoconductor.

Development

Charged toner from the developer gets attracted to the electrostatic image area that was created in the previous step due to the electrostatic field that is created. It is the most crucial stage in the electrophotographic process. Even though theoretical equations exist, most of the research is carried out using empirical techniques. The toner development occurs due to the force exerted on charged toner particles in the electrostatic field given by,

$$F = QE$$ Equation 1

Where,
F= Force acting on toner particle
Q= magnitude of charge of the particle
E= Electric field of electrostatic field.

This force dictates the motion of toner particles from the developer onto the photoconductor. The physics of toner development is a field in itself (Schein, 1999) and a detailed discussion is beyond the scope of this research.

Transfer

The toner developed on the photoconductor is transferred onto the sheet of paper (or onto a transfer belt prior to the transfer onto paper) which has been charged with a polarity of the opposite charge to that that was uses to charge the photoconductor.

Fusing

The sheet with selectively deposited toner is then passed through a heated roller, and the toner gets fused to paper under the combination of heat and pressure.

Cleaning

The excess toner on the drum is cleaned off the drum before beginning a new cycle.

EP-based rapid prototyping is still an unproven technology. There has been limited research that has been done in the field. The possibility of employing electrophotographic techniques to successively lay down multiple layers of material one after the other to construct a 3D geometry was first identified in the early 1990's (Bynum, 1992). The first working prototype of the process was demonstrated by Kumar (Kumar, 2000) of the University of Florida. Figure 4 is from Kumar's (Kumar, 2000) patent on solid freeform fabrication and it shows a schematic of the process that he first developed. Other researchers (Cormier et al., 2002; Jones et al., 2010) have contributed significantly towards the development of EP-based rapid prototyping. As seen in Figure 5, Jones et al. (Jones et al., 2011) have built the tallest samples (~10mm) produced by EP-based 3D printing. The research on EP-based 3D printing will be presented in greater detail in the literature review chapter.

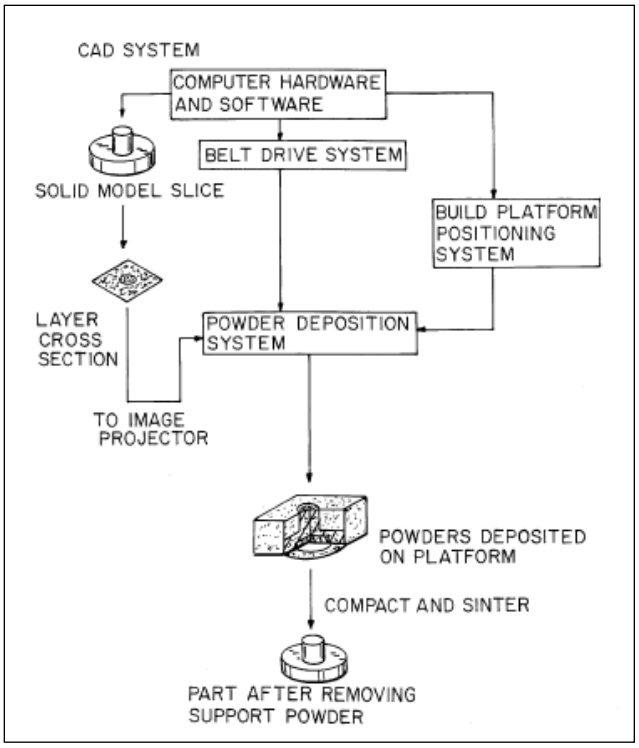

Figure 4: Solid Freeform Fabrication process (Kumar, 2000)

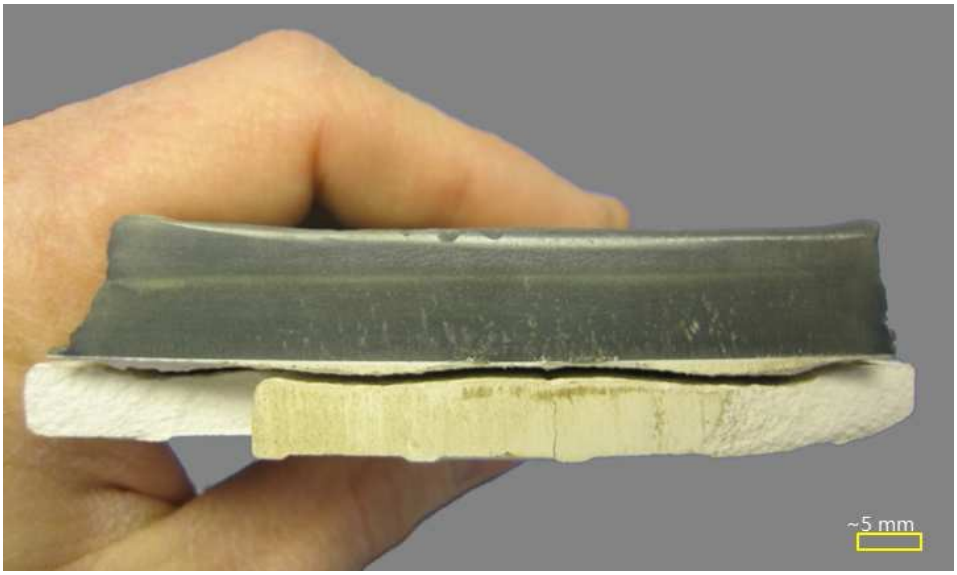

Figure 5: Tallest sample produced by electrophotography measuring 10mm (Jones, 2011)

1.2.1.2 Inkjet based rapid prototyping

Inkjet based color rapid prototyping involves the use of inkjet print heads to successively deposit multiple layers of material to build 3D parts. Based on the material being dispensed by the print head, the technologies can be categorized as follows

- Print heads selectively dispensing build material
- Print heads selectively dispensing binder over powder bed

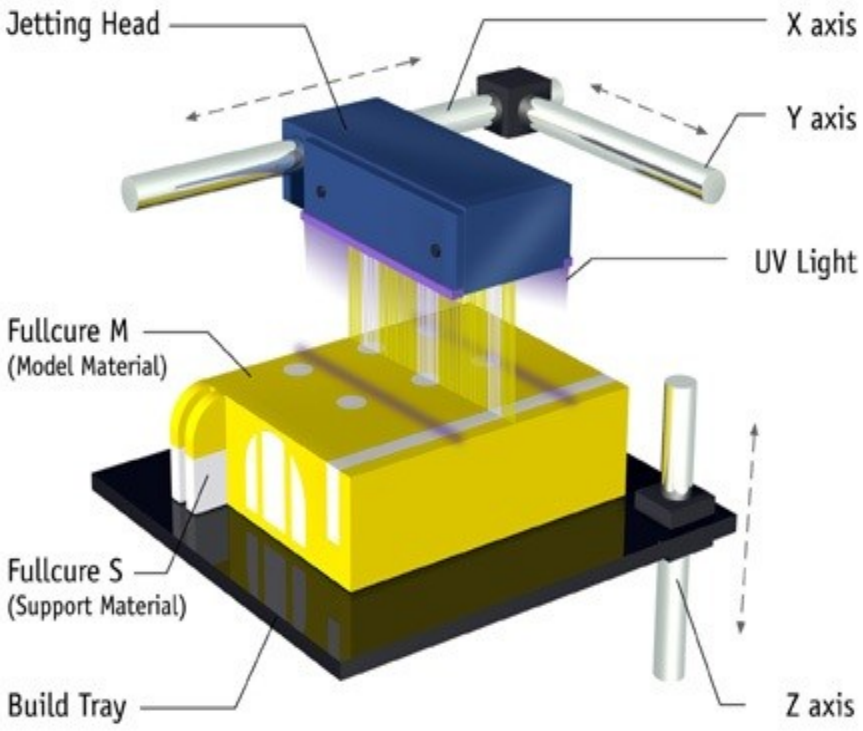

Figure 6: Objet Connex Process (Ref: Engatech)

Print heads selectively dispensing build material

The process directly prints photo curable resins on a substrate one layer at a time to create the 3D part. Each section is then cured using a light source which is usually a UV lamp. Cutting edge technologies today allow for multi-material printing to create a limited set of blended materials which can be different colors and can include support materials. Objet is among the industry leaders in this category.

Print heads selectively dispensing binder over powder bed

In this process, uniform layers with complete fill are deposited one after the other using a doctor blade. After each layer is spread, inkjet print heads selectively print a binder depending upon the geometry to be created in that layer. At the end of the build cycle, a part is formed that is held

together by the binder in a supporting bed of plaster-like material. The newly created part which has a limited green strength needs to be removed from the loose plaster-like material and needs post processing to increase the part strength. Further modification of the material properties is possible by infiltrating the part with a suitable material. Figure 7 provides a visual of the internal components of the ZCorp Z510 Spectrum.

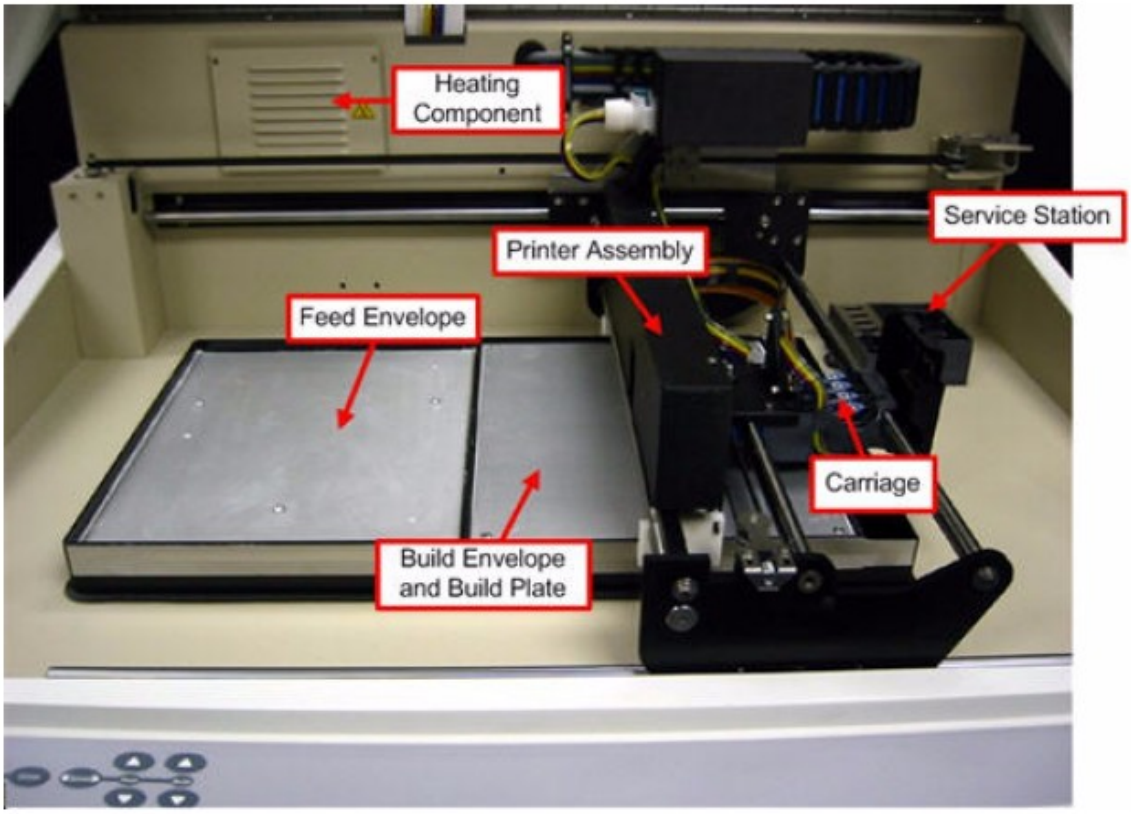

Figure 7: Internal Components of ZCorp Z510 Spectrum (Ref: User Manual)

Selectively colored parts can be created using this technology by using color principles such as half toning which are well developed for 2D printing. Z Corporation, which was recently acquired by 3D Systems, is the industry leader in using this technology. Z Corporation's 3D printers are currently the only commercially available rapid prototyping technology capable of producing selectively colored parts. Since ultimately this was the technology chosen for this study, details of this technology, in particular the Z510 model, were explored.

Z510 Spectrum

The following information is provided from product literature for Z510 Spectrum published by Z Corporation. Massachusetts Institute of Technology's patented 3DP technologies forms the core of Z Corporations 3D printers. First, software converts a solid model file into cross sections of required thickness. As seen in Figure 7, the printer includes two pistons - the feed piston and the build piston.

To print each layer, the build piston moves up by an amount equal to the layer thickness. The built piston simultaneously moves down by the same amount. A doctor blade then traverses from the feed piston to the build piston thus spreading a layer of powder. The excess powder is deposited in the chute designed for the purpose. Then, as the doctor blade returns to the original position, the print heads on the gantry print binder according to the cross section to be printed. The process repeats till the part its build. Powder that has not been printed upon surrounds the completed 3D part and provides support to features such as overhangs. Also, there is a service area to the left of the build piston which provides for periodic cleaning of the print heads.

In the next section, the controllable parameters of the Z510 Spectrum will be discussed.

Colors: The Z510 Spectrum features color rapid prototyping. Color is achieved using binder as the medium. The machine houses compartments for binders in four different colors, namely clear, cyan, magenta and yellow. Using the subtractive color scheme, the required color can be achieved for a given part. It should be noted that the part is colored only at the skin and has a white uncolored core.

Orientation: Referencing Figure 5, the axes of the machine are defined as follows:

X axis: It is the direction of motion of the overhanging gantry. For each position of the gantry along the X axis, the print head covers all the points along the Y axis.

Y axis: It is the direction that is perpendicular to the direction of motion of the print head, but in the same plane that is parallel to the powder bed. Relative to the motion of gantry along the X axis, motion of the print heads is faster along the Y axis.

Z axis: It is the depth of the build bed. It is the direction that is perpendicular to the plane that is parallel to the powder bed. Z motion is achieved by downward shifting of the piston within the build bed after the layer in the current X-Y plane is printed.

Depending upon the orientation of the part in the build bed, properties like the dimensional accuracy, color reproduction and the mechanical strength of the part change.

Saturation: The saturation determines the amount of binder applied per unit volume of powder and is represented as a percentage relative to the default 100%.

Bleed Control: This feature allows for the compensation for seepage of the binder through the powder due to spatial location and orientation in the build bed.

Powder: Over the years, Z Corporation has formulated increasingly superior powders to build 3D parts with higher green strength. Also, certain specialty materials have been formulated for infiltration by elastomeric materials for printing flexible parts.

Binder: Over the years, as with the powders, binder formulations have also been varied for better color reproduction. Currently, Z Corporation offers binders in four colors namely clear, cyan, magenta and yellow.

Layer Thickness: Typically, layer thickness affects the level of detail in a 3D printed part. Surface defects occur when a smooth slanted edge gets printed as a jagged edge which appears like a stair case. This defect is inherent due to the limitation of spatial registration for the print head along the Z axis because of finite layer thickness. There is a trade-off between the small layer thicknesses to achieve smooth finish for detailed features and having larger layer thicknesses for quicker builds. In the Z Corp process, layer thickness also determines the part strength due to the fact that binder is applied at every layer. Among other things, a postulate that will be tested in this research work is that layer thickness also affects the color reproduction in a powder-binder based inkjet rapid prototyping process like the Z Corporation's 3D printers.

1.2.2 Color Science

1.2.2.1 Overview

Since this research study is focused on color reproduction, a brief background of color science is useful. This section is based on materials that have been developed by (Berns, 2000; Wyszecki & Stiles, 1967).

Electromagnetic radiation has a broad spectrum of wavelengths. Human vision can perceive light of a small band of wavelengths from about 380 nm to 720 nm which is referred to as visible light. Any given natural source of light has a distribution of wavelengths associated with it. The dominant wavelength in the distribution determines the color of that particular source of light. The perception of color is the response to the stimulus to light of a particular distribution of wavelength impinging on specialized retinal cells in human eye. Specifically, there are three types of cone cells in the human retina which contains different pigments each sensitive to a different wavelength band. The cumulative effect of the responses of these different cone cells causes the perception of color within the human brain.

The importance of color in human life cannot be overstated. Color can be considered to be a composite, three-dimensional characteristic consisting of a lightness attribute and two chromatic attributes called "hue" and "saturation" (Hunter & Harold, 1987). The International Commission on Illumination (CIE) XYZ is the first color space that was developed in 1931 after a series of qualitative experimentation. Since then, many color spaces have been defined in attempts to improve upon the limitations of the previous spaces. Such color spaces are referred to as device independent color spaces.

CIE L*a*b* is an example of such a device independent color space. This color space is visually uniform with human perception. L* represents the lightness of color. The other two axes a* and b* represent the hue and chroma in a co-ordinate system. Positive a* is Red. Negative a* is Green. Positive b* is Yellow. Negative b* is Blue. The CIE L*a*b* or its polar transformation CIE L*C*H* (where L, C and H represents lightness, chroma and hue, respectively) are two of the commonly used color spaces to represent color measurements in this research. However for convenient representation

and computation, each device has its own color space known as device dependent color spaces such as sRGB and CMYK.

The RGB models produce colors by mixing red, green and blue light, with each color of light encompassing about one third of the visible spectrum. When red, green and blue light are combined, the whole spectrum of visible light can be reproduced, so the RGB model is known an additive color mixing model. To use the additive color model it is necessary that the object is itself a source of light. This is not the case with most of the objects surrounding us. Rather these are selective absorber of light. So a subtractive color mixing model was developed. Cyan is opposite of Red. Magenta is opposite of Green. Yellow is opposite of Blue. These Cyan Magenta and Yellow (CMY) are known as subtractive primaries. Conversely, mixing two subtractive primaries gives an additive primary.

Accurate reproduction of true Black is difficult using the addition of the subtractive primaries, so an additional Black toner has been added to the CMY toners to create a CMYK model for accurate reproduction of color in the printing industry. Similarly, other application specific or device dependent color spaces can be defined by mapping them to an absolute color space.

In a subtractive color model, the thickness of toner layer, the concentration of toner in the absorbing layer and its intrinsic absorbing properties determine the absorbance of light within the printed sample. The absorbance is different for different wavelengths of light. The selective absorbance in return determines the perceived color of a printed sample.

The next section provides an overview of the theories in color science that explain this effect in greater detail.

1.2.2.2 The Beer Lambert's law

Multilayer printing will result in substantial thickness of colorant to be deposited which will leads to the loss of intensity of light. The Beer Lambert's law states

$$A = -log_{10}(I/I_0) = \varepsilon cL \qquad \text{Equation 2}$$

It shows the relation between the absorbance of the material (A) with the extinction coefficient (ε) which is an intrinsic property of the absorbing material, concentration of the absorbing material in cross-section under consideration (c) and the thickness of layer (L). The absorbance is also a logarithmic function of the ratio of intensity of input light and the intensity of the emergent light. The sensitivity of human eyes to light is also a logarithmic function of light intensity, so it becomes easy to correlate absorbance to the perceived light intensity. The significance of this relationship is that in an effort to control color in a 3-dimensional solid, this loss of light intensity will be a significant factor that will need to be accounted for.

1.2.2.3 Kubelka-Munk Theory

The Beer-Lambert's law does not take into account the scattering of light in the medium. Of the many theories that can be used to account for the absorbance as well as scattering of light, the

Kubelka-Munk theory is the most popular. According to the stated theory, the solution to reflectance factor (R) and transmittance (T) is provided in terms of four parameters, namely scattering coefficient (S), absorbance coefficient (K), thickness of layer (L) and the reflectance of material behind the layer (R_g). Thus,

$$R = f_1(S, K, L, R_g) \quad \text{Equation 3}$$

$$T = f_2(S, K, L, R_g) \quad \text{Equation 4}$$

A specific condition of 'complete hiding' occurs when the layer of material is so thick that it reflects the same amount of light with a background R_g=0 as well as R_g=1. Applying specific boundary conditions to the system, the Kubelka-Munk equation can be represented by

$$\frac{K}{S} = \frac{(1 - R_\infty)^2}{2R_\infty} \quad \text{Equation 5}$$

When this equation is solved for R_∞, it yields,

$$R_\infty = \frac{S + K}{S} - \sqrt{\left[\left(\frac{S + K}{S}\right)^2 - 1\right]} \quad \text{Equation 6}$$

This expression results in the fact that the reflectance factor for a layer at a depth greater than the depth of the complete hiding thickness is constant and equal to the reflectance factor for the complete hiding case. This bounds the research to investigate color reproduction only up to the depth equal to the thickness at the complete hiding case.

1.3 Summary

In this section, the value and importance of color in 3D structures has been motivated. In addition, the basic fundamentals of Rapid Prototyping have been introduced. More specific overviews of EP-based rapid prototyping and ink-jet-based rapid prototyping have been presented. Finally, important color science principles relevant to this research work were introduced. In the next section, the state-of-the-art in characterization of color performance of rapid prototyping processes will be presented.

2 Literature Review

In this section, research that has been conducted in EP-based rapid prototyping and in inkjet based rapid prototyping will be reviewed.

2.1 Electrophotography based color rapid prototyping

The US patent 5088047 (Bynum, 1992) was the first patent to suggest the use of electrophotography as an additive manufacturing processes. Since then, a few research groups have tried to develop processes to implement the process but only with limited success. Developing a commercial EP-based rapid prototyping process has remained to be an elusive goal (Grenda, 1996) (Cormier et al., 2002) (Kumar & Dutta, 2003). The challenge of the loss of luminescence in selective coloring of 3D structures using electrophotography had been identified in 2002 (Cormier et al., 2002). The fundamental difficulty of compensating for the loss of luminescence with multiple color layers was tackled by building a white core with a single colored skin layer (Cormier et al., 2002). Nonetheless, laser printing of 3D objects holds great promise because of its potential of very high printing speeds compared to other rapid prototyping technologies. Further, laser printing is a mature technology in the world of 2D printing, and this is a knowledge pool that can be leveraged to develop the 3D technology. One of the most significant challenges that must be solved is the development of functional materials that can be transferred without a height limitation for the fabricated part (Jones et al., 2010; Wimpenny et al., 2008).

It is evident that the development of a commercially viable EP-based rapid prototyping process is still a long term research vision. Achieving such a vision will require developing capital intensive equipment, adapting the very specialized and empirical process knowledge of electrophotography to 3D applications, and intensive material science research to develop suitable functional materials. Currently, only a couple of research groups around the world namely, XActiv under the Torrey Pines research umbrella and DeMontfort University in United Kingdom are actively pursuing this research.

However, even with these daunting hurdles that must be overcome, integration of color into rapid prototyping is of great value, as was discussed above. It was also noted that to make rapid prototyping a mature communication media, color is required to accurately convey information (Rees, 1998). Thus, reproducing the desired color is as much of an interest in EP-based rapid prototyping as any other process, and it would make the process more robust in addressing the needs of the prototyping industry.

2.2 Inkjet based color rapid prototyping

The first work to demonstrate selective coloring in rapid prototyping was for a selective laser sintering process using ink-jet printing (Ming & Gibson, 1999). Inner visible multi-color prototype fabrication has been successfully demonstrated using stereolithography (Im et al., 2002).

Today, the only commercial available rapid prototyping systems to accomplish selective coloring are the Z Corp 3D printers which 3D color print only at the outer skin layer. The first work to study color accuracy described the effect of orientation and post-processing on the measured color difference of

3D printed part (Parraman et al., 2008). Color differences were measured using a Gretag Macbeth Eye One in the CIEL*a*b* color space. The research studied the color difference of 3D printed part before and after infiltration with paraffin wax. From a visual perspective, layer stratification on the vertical faces of the part and mottled appearance due to texture on the upward facing surface of the part was observed. A slight darkening effect was also identified upon infiltration with wax. The study recommended further research to incorporate the measured color differences to improve screen based design and visualization tools to enable designers to have a finer control over the color accuracy of 3D printed parts.

The impact of infiltrants on the mechanical properties of 3D printed objects and on their surface appearance was studied ((Lozo et al., 2008). The Z Corporation's Z510 Spectrum was used in this study along with zp130 powder and zb58 binder. The different samples were infiltrated with cyanoacrylate, epoxy resin and polyurethane by completely dipping the sample in the infiltrant fluid. Tensile strength was measured using a universal tensile testing machine to record the tensile strength at break; a Charpy impact type impact apparatus was used to measure the impact strength; and a hardness test was conducted using the ball indentation method. The effect of each of the three types of infiltrants was documented. Gravimetric measurements showed a 21% increase in weight in the sample infiltrated by epoxy agent, 12% increase with a cyanoacrylate agent and 7% with a polyurethane agent. Compared to a non finished sample, epoxy agents were found to increase the tensile strength 5.23 times, cyanoacrylates by 2.77 times and polyurethanes by 2.32 times. Also, surface properties were measured by visual inspection, optical microscopy, and by using a scanning electron microscope (SEM). It was found that infiltration by epoxy resin and cyanoacrylate led to smoother surfaces. It was also found that the polyurethane infiltrated surfaces resembled the untreated samples.

The impact of the infiltrants on color reproduction was also studied (Lozo et al., 2008). Based on infiltration method, the samples were categorized as untreated, treated with cyanoacrylate based Z-Bond, and epoxy based Z-Max. The article establishes the basic color measurement methodology for 3D printed samples. A spectrophotometer was used to study the color reproduction of additive and subtractive primary colors in addition to black and white. The color measurements were performed using a CIE L*c*h* color space. Post processing with infiltrant caused a decrease in lightness but an increase in the saturation of the color. Also Z-Bond infiltration led to a higher increase in saturation than with Z-Max.

A technical comparison of the color reproduction performance of two 3D inkjet color printers was performed by (Walters et al., 2009), which studied the effect of two commonly used infiltrants, namely cyanoacrylate and paraffin wax. Twenty-four color test blocks based on the color checker classic chart of Gretag Macbeth were chosen to represent a good range of colors and grey tones. A set of samples were printed using each Z510 and Z650 color 3D printers using zp131 powder and zb60 binder. The parts were sanded and infiltrated with either wax or Z-Bond. Color measurements were taken on the top, front, side, and curved surfaces using a Gretag Macbeth Eye One spectrophotometer with D50 illuminant and the measured data with specular included was saved in

CIE L*a*b* format. The effects of infiltration and of different surfaces were studied. It was noted that the effect of banding on vertical surfaces and the stair-step effect on angled or curved surfaces could be alleviated by sanding the parts prior to infiltration. Based on the difference in color reproduction with varying post-processing methods, the research demonstrated the need to develop color profiles for each finishing method. It was noted that the slight gloss of ZBond creates an appearance of homogeneous color. Both types of infiltration were also noted to reduce the appearance of stripes on the surface.

The print reproduction in rapid prototyping was studied by (Stanić et al., 2010). The research characterized the effect of shell saturation level, bleed control, location and orientation in the print bed. In one experiment, the research studied the effect of position of the part in the print bed. In another experiment, the orientation, shell saturation and bleed control were varied to study their effect. The Spectrum Z510 was used to perform the experimentation using zp131 powder and zb60 binder. Following printing, the loose powder on the sample was cleaned, and images of the same were captured using Leica EZ4D stereomicroscope. The image analysis was performed using IMAGEJ software. A threshold color plug-in was used to distinguish between the region of interest and the background in RGB channels. The difficulty in objective analysis was noted due to rough uneven topography. Circularity which is a measure of difference of 3D printed circle from an ideal circle along with other metrics like total area, perimeter, feret diameter and major and minor axes were used to study print accuracy. It was also noted that stripes are visible on vertical surfaces as well as solid colored areas.

Colorimetric properties and stability of 3D ink jet prints has been discussed by (Stanic et al., 2012). 3D color samples printed on Z510 Spectrum using zp131 powder and zb60 binder and categorized as untreated, finished with cyanoacrylate based infiltrant and finished with epoxy resin based infiltrant. The samples were placed under Xenon-Arc based weathering apparatus to test color stability under an accelerated aging procedure. A Gretag Macbeth XTH spherical geometry spectrophotometer was used to measure spectral reflectance under varying wavelengths using a D65 light source, and the measured data were converted into CIEL*a*b* color space. Analysis showed that changes in the color appearance with varying finishing methods could be mostly attributed to the changes in chroma and lightness. Stability of samples was also shown to be dependent upon the color, ink coverage and finishing method.

Even a non functional prototype for aesthetic purposes needs adequate mechanical strength to withstand environmental and handling stresses. So, for practical applications, mechanical strength is an important criterion that can impact the choice of process parameters. The effect of layer thickness and binder saturation on the properties of inkjet 3D printed samples has been studied by (Vaezi & Chua, 2011). Dimensional accuracy, tensile strength and flexural strength of uninfiltrated green parts printed using a ZCorp Z510 were studied. At a constant layer thickness, increased binder saturation was observed to increase the mechanical properties of the part and maintain consistent surface quality. Also, at constant binder saturation, decreased layer thickness was observed to increase the

mechanical properties of the part but resulted in the deterioration of the surface quality and uniformity.

2.3 Summary

In the literature review, the state of the art research in EP-based rapid prototyping and ink jet based rapid prototyping has been discussed. The development of EP-based rapid prototyping from the initial conception by Bynum in 1992 to the first working model developed by Kumar has been discussed. Cormier's successful demonstration of color rapid prototyping using electrophotography was discussed in detail. Further research in increasing build thickness and research on toner materials by Wimpenny was also described.

In addition, implementation of inkjet printing for 3D printing was reviewed. Special attention was given to the Z Printer since it is capable of selective coloring in 3D ink jet printing.

3 Problem statement

3.1 Initial Investigation

In the previous chapter, the importance of color has been motivated. In order to characterize the color performance, it was first necessary to demonstrate that we could, in fact, manipulate a mixture of color powders and measure a corresponding change in color performance. In this section, three different experiments to illustrate this control will be described.

3.1.1 Die press toner

In Electrophotographic printing, fusing takes place by application of heat and contact pressure. Non thermal fusing is also feasible, however it requires high pressure and may cause substrate deformation. The above observed effects were not the immediate concerns towards building color 3D structures. So, using a simple die-punch set in RIT's Brinkman Lab, pressure based fusing of dry magenta toner was carried out. Two different types of experiments were conducted using die pressing. The first experiment was to determine how the color values are affected by thickness of toner disc. The second was to determine how the color values are affected by mixing white powder in color toner.

Study effect of thickness of toner disc on the color values

A weighed sample of dry magenta toner was placed in a 15mm die cavity. The die set was shaken by hand to ensure uniform distribution of toner across the surface of the die. The punch was then placed in the die cavity and compressed to a pressure of 6MPa. The pressure was maintained for about 10 seconds and then released. The disc was then carefully removed, and the color values were measured using an X-Rite 508 spectrodensiometer.

A spectrodensiometer is an instrument designed to measure color in terms of optical density. The X-Rite spectrodensiometer is a handheld device was used to measure the color in 4 color density values. The measurement is done in terms of optical density (D). Optical density is defined as the log of reciprocal of transmittance. For the equipment used, the measurement range was 0.00D to 2.5D.

Based on the measurements, it is evident that die pressed discs maintain their color values with increasing thickness. The observations can be explained using the limiting case of the Kubelka Munk model which explains how a thick system reflects the same light irrespective of background reflectance. The complete hiding thickness is achieved after a certain number of layers when the component of light being transmitted through the thickness of the disc and reflected back by the white background is negligible. Thus, the reflectance of the top toner layer behaves independently from the reflectance of the underlying substrate. As a result, the values recorded are now the values of the component of light reflected from the toner layers up to the depth of complete hiding thickness.

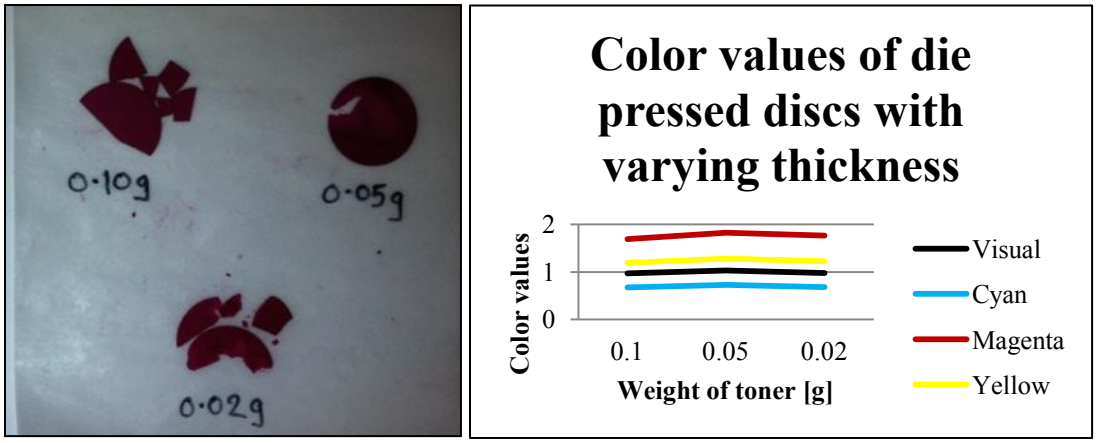

Figure 8: Die press color disc samples and their color values measured using spectrodensiometer

Study on the effect of mixing white to the color toner on the color values

This experiment was performed using the same apparatus. Potato starch powder that is white in color was used for its easy availability and its comparable particle size. Sample mixtures weighing 0.05 gm were prepared with varying proportions of magenta toner and starch by weight. The experimental observations were noted, and the results were analyzed to find whether there was any compensatory effect of white toner to the change in color values with the increased thickness of toner. It was found that smaller color values were obtained when a blend of white toner and magenta toner was used rather than 100% magenta toner.

However, the mechanism of die-press fusing and that of electrophotographic printing are different. In order to determine whether or not similar results would be achieved using electrophotography, the experiment would need to be performed using a process which has a fusing mechanism more closely related to laser printing.

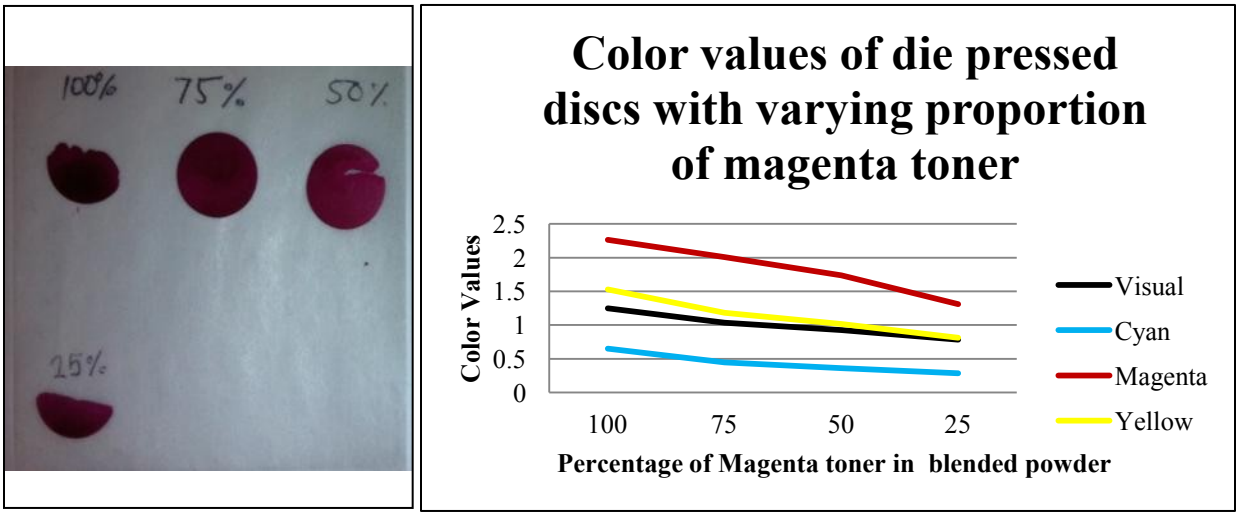

Figure 9: Control over color values of die pressed discs by controlling the percentage of toner

3.1.2 Coupon stacking

Post-Script code was used to print a 100% fill of magenta toner on a letter size transparency. This transparency was then cut into 1inch by 1.5 inch coupons. The color values of stacking coupons were measured using an X-Rite 508 spectrodensiometer. Also, the luminosity measurements were taken using a lux meter. The loss of luminosity respectively in the measurement due to the transparency itself was compensated for by repeating the experiment with a set of stacked coupons of unprinted transparency.

However a commercial color printer adds a pattern of yellow toner to each print that is developed through it. This is done to verify the authenticity of any print and to prevent counterfeit print samples. For security concerns, there is no software unlock for this feature. As a result , color analysis done on prints generated out of such a printer are skewed giving higher than expected values of yellow. Secondly, even though an attempt was made to compensate for the effect of multiple transparency sheets, each coupon of transparencies creates an intermediate transparency-toner interface and another transparency-air interface leading to differentials in absorption and scattering. Characterizing the effect of such interfaces as light passes through them is beyond the scope of this study.

Nonetheless, this experiment confirms with the observations of the selective coloring experiment that multiple layers of toner do not affect the hue of the color, however they cause a loss in the luminosity of the perceived color.

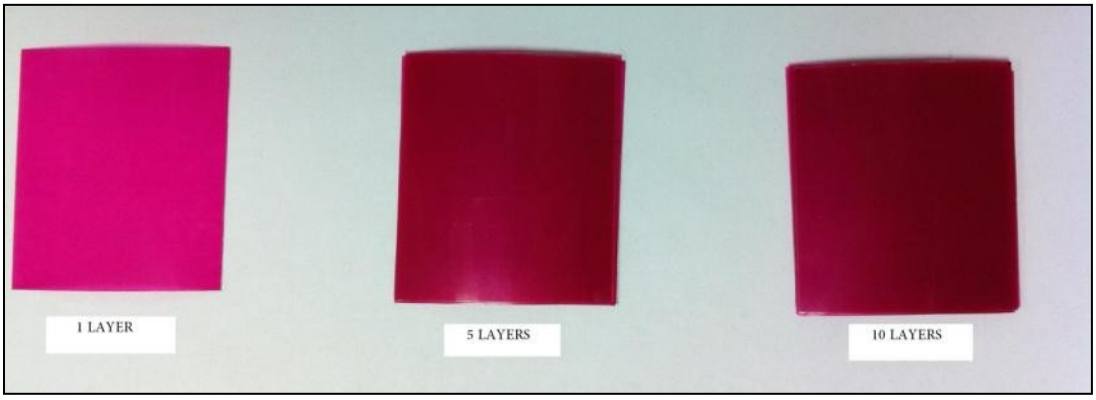

Figure 10: Visual perception of difference in color due to loss of luminosity with increasing number of layers

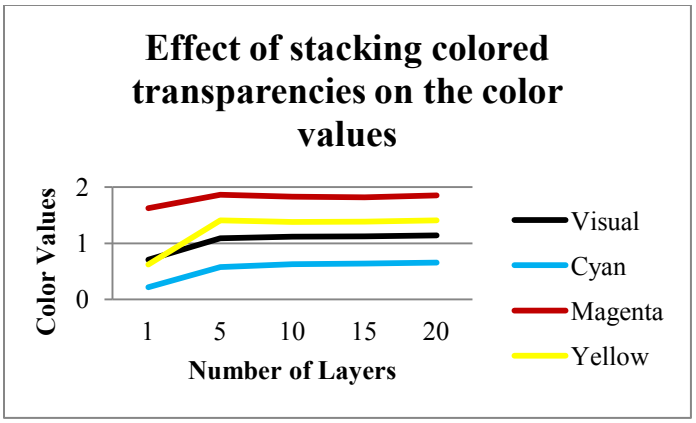

Figure 11: Constancy of color values with increasing number of layers

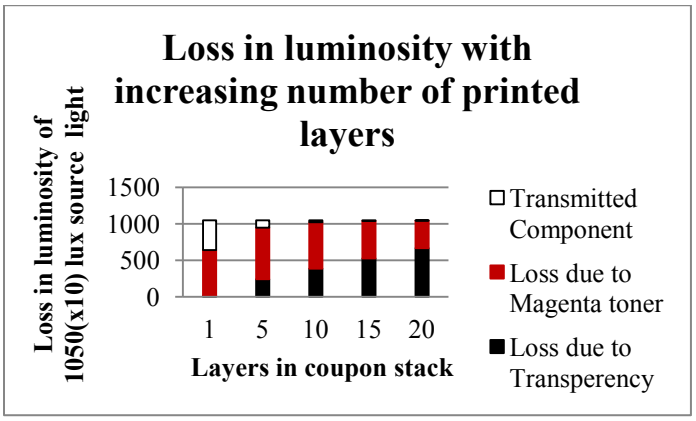

Figure 12: Loss of luminosity due to increasing layers

3.1.3 Adapted Commercial Laser Printer

An attempt was made to improve the level of performance of the samples by using a commercial laser printer. The difficulty faced in this approach was that laser printers have an upper limit to the height that can be built on paper. Beyond this height, the electrostatic field required for successful toner development is not maintained, resulting in unacceptable development characteristics. The primary reason can be attributed to inadequate charging of the substrate because the substrate is no longer paper, but is rather the surface of a previous layer of deposition. This layer is not only further away from the charging plate but also is made of toner, causing much difficulty to characterize the required electrostatic field as a function of increasing thickness of deposition of cumulative layers (Kumar & Dutta, 2003). A solution was found to this challenge by printing toner without fusing onto a silicon coated Mylar substrate and then manually transferring it to a separate substrate. It can then be fused on a separate roller fusing bed. However, the samples generated by this process suffered image registration problems due to the manual handling that was required. Also, the process was labor intensive, requiring two days for depositing 25 layers of toner to build up a height of about 70 micrometers. Also, as previously observed (Jones et al., 2010), an increase in the number of layers led to an increase in surface defects.

Previous experiments demonstrated that it is not feasible to develop a process to deposit multiple layers of material without investing resources in development of a dedicated test bed. So it became necessary to develop a testing procedure to study the effect of depositing multiple layers of color toner that do not require actual toner development using electrophotography.

Knowing that color reproduction is the primary effect under study, and given the constraint of not being able to print in 3D, two separate non EP based solutions were identified and investigated.

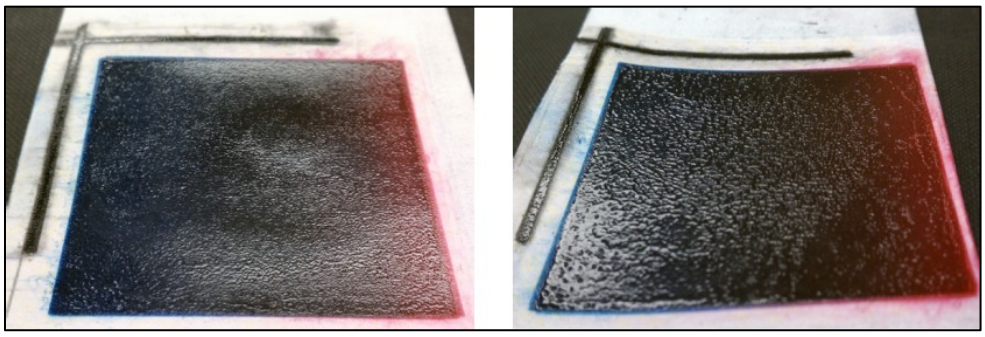

Figure 13: Surface irregularities with 15 layers (L) and 25 layers (R) when deposited using an adapted commercial laser printer

3.1.4 Summary

Based on the feasibility analysis, it can be seen that control over color reproduction involves many factors including thickness of the color layer, saturation of color and number of layers. These factors have been represented visually in Figure 14. However, with multilayer printing there are chances of surface defects. Ideally, our selection of experimental process needs to offer control over most if not all of the significant factors involved in color reproduction. At the same time, the process needs to be robust enough to obtain reproducible results with minimal surface defects that could potentially distort the findings of our final experiment.

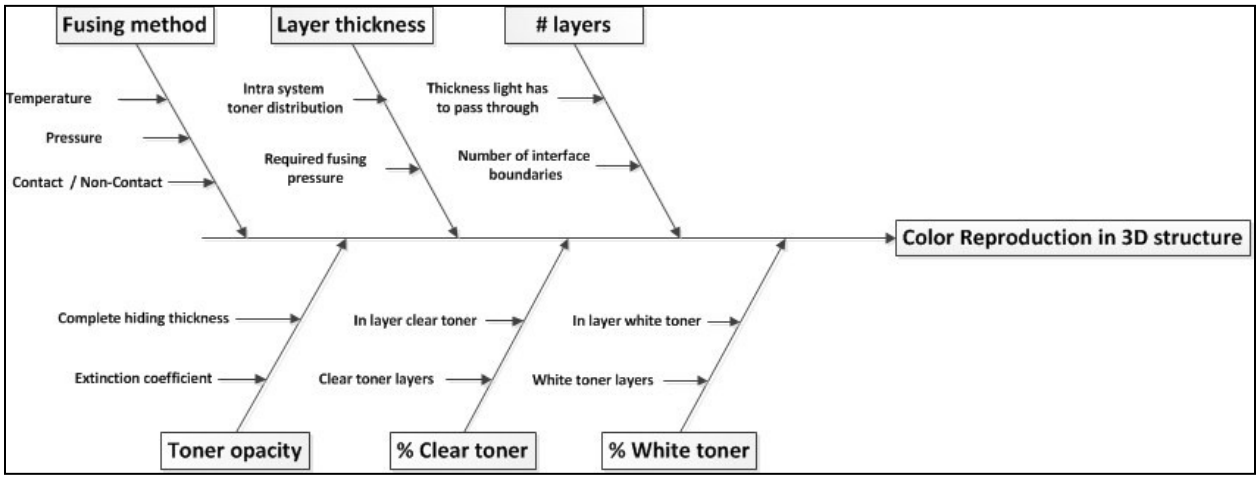

Figure 14: Ishikawa diagram of the factors influencing color reproduction in 3D printed structures

3.2 Research Objectives

The long term goal of this research is to integrate full color into 3D structures created by rapid prototyping. This means the reproduction of the desired color at a given spatial location within parts that are custom designed and manufactured on demand. To accomplish this vision, however, requires a great deal of research on various aspects including the development of 3D printed surfaces with high tolerances, the interaction between powders and binders, the development of knowledge to set the process parameters to the reproduced desired colors, and the materials knowledge to achieve the required performance characteristics, such as mechanical strength, to name a few. Much of the above mentioned research requires detailed material science and color science knowledge and is beyond the scope of this research work.

As a result, the immediate focus of this work is to characterize the effect on color reproduction of the interaction between powders and additives to the powders as a function of various layer properties. From the literature review performed and the initial experiments described above, it is reasonable to conclude that number of layers, the layer thickness, how the pigments are introduced and mixed, and how the layers are bound together will have an effect not only on the color performance, but on the functional performance of the part. Thus, the objectives of this research were divided into an exploratory phase and an experimental phase.

Exploratory Phase

- Explore methods to experimentally mix and bind powder that will yield process insights into color reproduction for EP-based and/or inkjet based rapid prototyping
- Given the results of the exploration above:
    - Select an experimental approach
    - Define an experiment and the appropriate process parameters will yield information about color performance and functional performance

Experimental Phase

The exploratory experiments that were performed in response to the aforementioned goals are described in detail in Section 4.1. As an outcome of that process, an inkjet-based rapid prototyping experimental set-up was selected for further investigation. The focus in this experimental phase is the design of a factorial experiment to study the effects of the relevant process parameters on the color reproduction in the 3D structures. With the data generated from the experiment, an empirical model to characterize the variation of color in response to changes in the levels of each of the significant control parameters will be generated.

The specific goals of this experimental phase of the study were the following:

> Study the effect of layer thickness on the color, gloss and mechanical performance of 3D printed structures - as the layer thickness is varied, the rate of binder dispensed per unit volume of powder changes. It is suspected that changing other related factors including the

time allowed for the binder to adhere to the powder, the magnitude of binder penetration in the part, and the number of binder droplets dispensed per unit volume of powder could influence color response. Initial experimentation confirmed that layer thickness is a significant factor in determining the color reproduction in 3D printed ink jet samples.

Investigate interaction effects of layer thickness, binder saturation, infiltration and color - various factors like hue, shell saturation and infiltrant have been previously researched in individual studies. As an integrative effort, the research will study the control factors in a factorial design experiment to discover the interaction effects, if any, within the factors along with their primary effects. The estimates of interaction effects discovered in the systematic experimental methodology will lead to better understanding of the color reproduction in rapid prototyping.

Explore the tradeoff between color, gloss and mechanical strength - as a part of the experimental methodology, tensile testing of specimens would be conducted. Along with the color reproduction study, this would help in developing response surfaces to determine the required processing and post-processing parameters to achieve the required balance between accurate color reproduction on a wide gamut of color and the mechanical strength required to maintain structural integrity in the envelope of the operational environment. Insight into this topic has high value in the sector of functional prototypes where trade-offs need to be made between the required appearance characteristic and the required mechanical strength of the part.

An outcome of this research will be a linking of research activities in rapid prototyping, color science and the print industry. It is believed that such an association would aid in the growth of rapid prototyping as a commonplace commercial technology.

4 Research Methodology

4.1 Exploratory phase

Since our goal was to study color, one way to achieve this would be through mixing of different color powders. This approach would be better suited for EP-based RP. On the other hand, for inkjet based RP, the colorants can be delivered through the binder. As a result, a variety of approaches were considered. To mimic EP-based RP, the objective was to find methods to generate thin uniform layers of a particular powder mixture. These approaches included direct transfer of toner to charged paper and tape casting. They will be discussed in greater detail below. For ink-jet based RP, since this was a mature technology, the Z Corp platform was ideally suited for this study. However, we would lose the ability to control the number of layers with colorant in them, thus limiting our original study.

4.1.1 Direct transfer of toner to charged paper

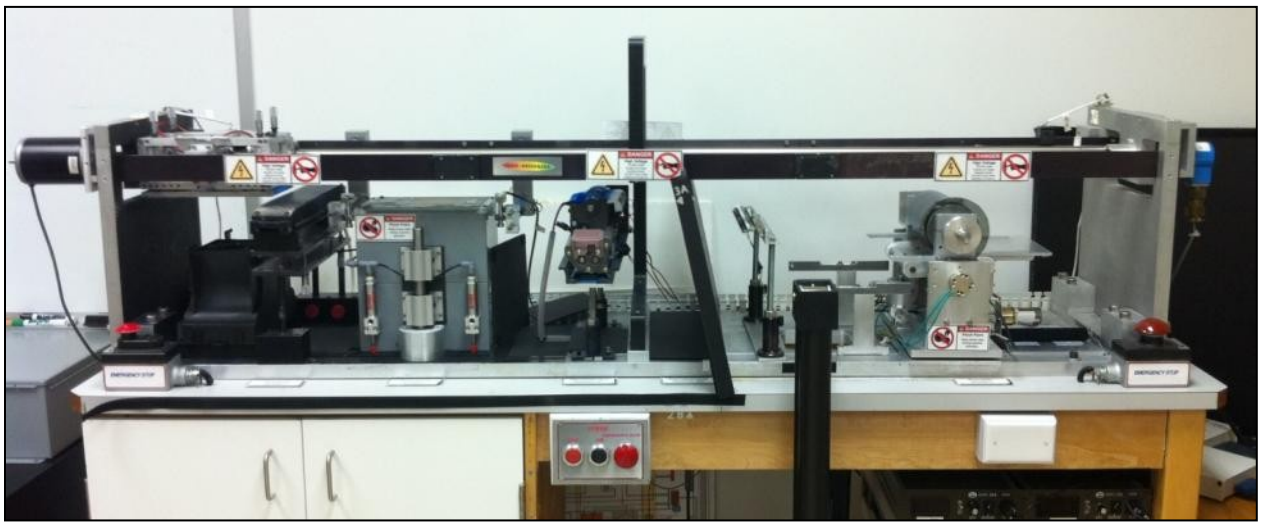

Figure 15 : EP test bed setup

The most crucial stage in EP printing is the development stage. It is difficult to develop a deposition process without a full understanding of the material to be deposited and the electrostatic physics behind it. A modification of the standard laser printing workflow was conceived to bypass the development and transfer stage. Paper was charged directly using the electrophotography test bed. Without the photosensitive polymer, it was not possible to create an image so the development proceeded to create a complete fill. A glossy paper with polymer coating was used to allow accumulation of charges on the surface of paper. As seen in Figure 16 the initial results were promising.

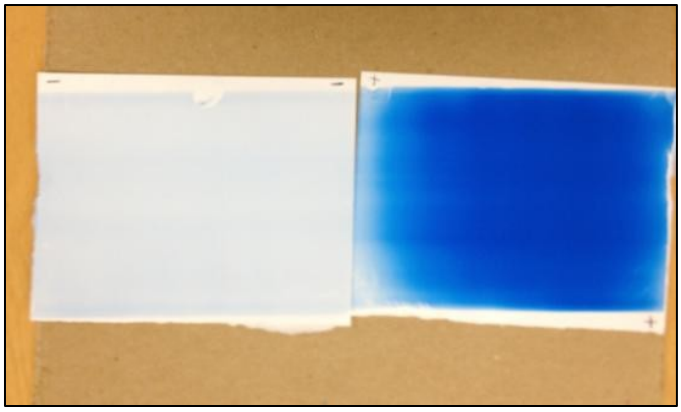

Figure 16 : Direct transfer of toner to charged paper

4.1.2 Tape casting

Tape casting is a technique which was initially used in the paint industry to test the covering power of paint formulations. As seen in Figure 17 the basic technique consists of depositing the powder of the material to be formed, known as slip, through a measured slit between the doctor blade and the underlying surface. Mechanical force is applied to drag this assembly across the substrate thus forming a thin film of deposited material on the substrate. This is then subjected to post processing using a heating enclave or similar approach.

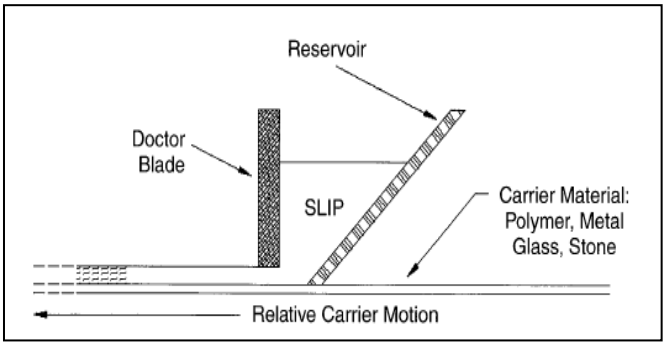

Figure 17: Illustration of tape casting (Ref: Mistler and Twiname, 2000)

Using this process, the magenta toner was laid on a polymer substrate. The sample was prepared by dragging the doctor blade manually across the substrate leaving a 25.4µm gap to deposit the toner. A heat lamp was used to fuse the toner to the substrate. The dry toner did not fuse well. Initially water was used as the carrier medium for the toner, however the toner was immiscible in water and floated to the surface. Isopropyl alcohol was then tried as the carrier medium for the toner with the expectation that it would evaporate once deposited. Isopropyl alcohol wetted the toner particles and formed a slurry. The fusing seemed to be better when this slurry of toner in isopropyl alcohol was used. The possible cause of this could possibly be due to the improved heat convection through the liquid medium of isopropyl alcohol. A sample generated by this method is shown in Figure 18.

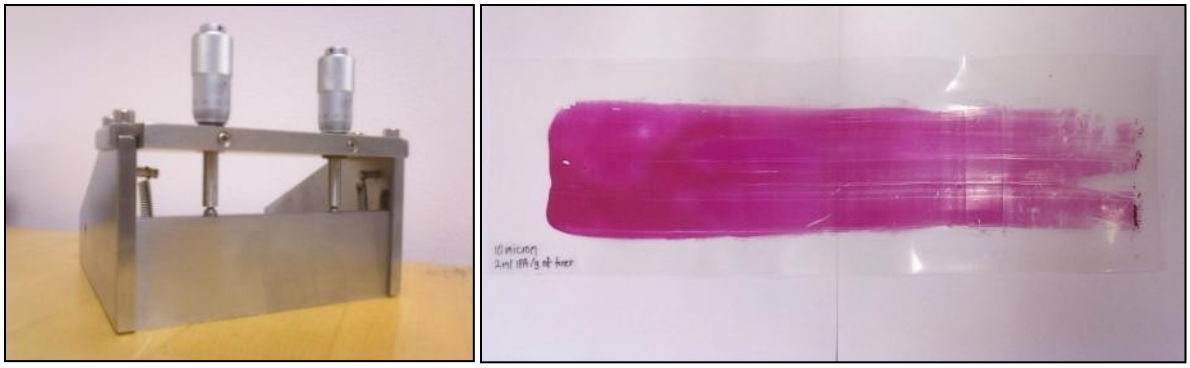

Figure 18: Tape Casting apparatus and sample deposited by tape casting

4.1.3 Z Corporation 3D ink jet printing

Z Corp 3D Printers are the only available commercial technology capable of reproducing selective color. The process details have been previously covered in Section 1.2.1.2. The only limitation of this process is that it is not possible to control the number of color layers. However, as the technology has already been commercialized, tight process controls have already been developed and implemented. It provides a platform to conduct effective experimentation with a much higher degree of control over the noise factors existing in aforementioned methods of toner transfer. Some of the parameters of process control in the Z Printers have already been characterized. However, previous literature highlights areas that warrant further exploration.

As part of our exploratory investigations, color response of Z510 Spectrum was studied as a function of layer thickness. Two samples with the exact same input color, defined [255, 0, 0] in the RGB color space, were printed at two different layer thicknesses of 0.1mm and 0.089mm as seen in Figure 19.

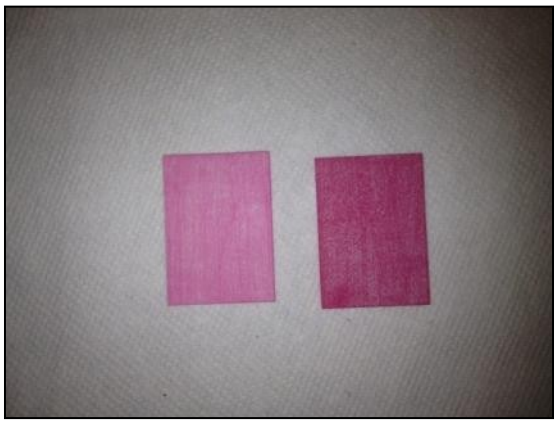

Figure 19: Difference in color reproduction due to change in the layer thickness from 0.1mm (L) to 0.089mm (R)

4.1.4 Results of the exploratory phase

The initial results of direct transfer of toner on charged paper were promising. However, the process exhibited very limited repeatability and it was very sensitive to environmental conditions like

ambient humidity. Due to the available equipment, one of the biggest drawbacks was the lack of multicolor development. The EP test bed had only one development station. The research would be severely limited if the experiment were conducted using this process.

Tape casting was a very robust process allowing control over layer thickness and material mixtures. However, preparation of inks and control of spreading ability of powders was a challenge. Each toner material necessitated a new ink formula. These inks were not very stable, and their characteristics varied over time. For certain material sets like thermosetting polymers, conventional roller based fusing was inadequate to fuse the toner to the substrate, and suitable equipment was not available to pursue further research.

The study of color reproduction in a more controlled process is required to further explore the preliminary observations. Even without control over the number of layers, the ink jet 3D printing process for generating samples is a more repeatable process and offers adequate degrees of freedom for experimental purposes. The color response to change in layer thickness in 3D ink-jet printing process had not been studied previously and warranted further experimentation.

Based on the results of the exploratory phase, a decision was made to choose the Z Corp Z510 Spectrum as the process to generate further experimental samples.

4.2 Experimental Phase

Based on the research objectives stated in Section 3.2, experiments were conducted to characterize color reproduction, mechanical strength and wetting characteristics of 3D printed samples.

4.2.1 Factorial Design of Experiment to characterize color reproduction

4.2.1.1 3D printing

The main aim of the research study is to characterize the color reproduction in rapid prototyping. A factorial experiment was designed to vary the control factors orthogonally. The samples were printed using Z Corporation's Z510 Spectrum ink jet rapid prototyping machine using zp150 powder and zb60 binder. Throughout the experiment, the bleed control was kept off. The layer thickness, as a control factor, was held at three levels 0.089mm, 0.100mm and 0.114mm. In order to study the color response across the color spectrum, each of the subtractive primary and secondary colors were studied at coverage level of 15%, 60% and 100%. Further, the binder saturation was another control parameter held at 85% and 100%. Finally, infiltrant was the last control parameter studied, and it was held at 5 levels consisting of 4 different infiltrants and one set of samples which were uninfiltrated. Six batches of specimens measuring 30mm x 30mm x 4mm with varying hues and color saturations were 3D printed at a given shell saturation and layer thickness one after the other.

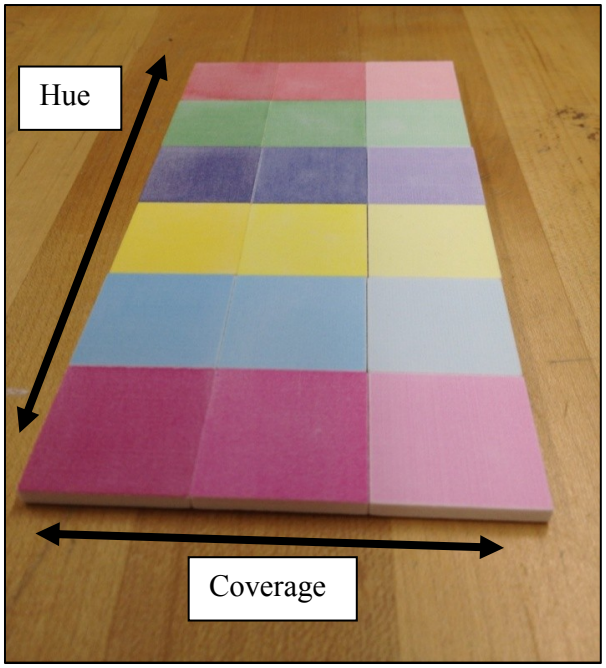

Figure 20: A batch of color samples

The color specimens, as seen in Figure 20, were then infiltrated with various infiltrants as shown in Table 1 by submersing them completely in a bath of infiltrant for 1 minute. Excess infiltrant was drained off, followed by air drying of the samples overnight with the color surface facing upward. The table below depicts the various control factors in the experiment held at discrete levels.

Table 1 : Experimental Factors and their control levels

Layer Thickness	Infiltrant	Coverage (%)	Hue	Binder Saturation
0.089mm	Z Max 90	15	R	85
0.1mm	EpoxAcast 690	60	G	100
0.114mm	EpoxyAmite 103	100	B	
	West System Epoxy		C	
	Uninfiltrated		M	
			Y	

Detailed information about each of the infiltrants is provided below. The other control factors have been described previously in Section 1.2.1.2 and Section 1.2.2.1

West System Epoxy Resin

105 Epoxy Resin: It is a clear pale yellow liquid epoxy resin with a viscosity of approximately 1000cP at 22ºC. It does not contain any volatile solvents, so it does not shrink after curing. It is a versatile epoxy and can be used with wood fiber, fiberglass, reinforcing fabrics and a variety of metals. When used with a 207 Hardener, it is claimed to cure clear.

207 Special Clear Hardener: It is a clear moisture resistant hardener developed for coating and fiberglass cloth applications. When used with 105 Epoxy resin, it is claimed to reach adequate strength for structural purposes and laminating coats. It is recommended that it be used in a ratio of three parts of 105 Epoxy resin to 1 part of 207 Hardener for optimum strength. It has a pot life of 20 to 26 minutes at 22ºC. A cure to solid state takes 10 to 15 hours.

EpoxAcast 690: It is a clear casting two component epoxy resin system made available by Smooth-On. It is advertised to be suitable for rigid clear finished product and is claimed to have negligible shrinkage, high strength and hardness on cure. It is also suitable for creating clear encapsulations for electronic components. The epoxy is recommended for thicknesses up to 50mm. The Part A and Part B are recommended to be mixed in 10:3 ratios by volume to achieve optimum cast properties. It has a pot life of 5 hours. A complete cure to set takes 24 hours.

EpoxyAmite 103: It is a low viscosity odorless room temperature curing epoxy system which is clear yellow in color. It is advertised for its high physical and performance properties. It is designed to be used as a reinforcing system for composite parts. The Part A and Part B are recommended to be mixed in 3:1 ratio by volume to achieve optimum cast properties. It has a pot life of 55 minutes. A complete cure to set takes 20 to 24 hours. While the epoxy system is not clear, curing it exhibits very good mechanical properties and thus was introduced in the experiment as a benchmarking reference for mechanical tensile testing.

ZMax 90: According to Z Corporation, the ZMax 90 is a low viscosity high strength binder designed for broad spectrum needs from display prototypes to functional parts.

Each infiltrant needs certain ratios of part A and part B to achieve desired properties. The ratio of each infiltrant is provided in Table 2.

Table 2: Ratio of Part A resin and Part B hardener in various infiltrants

Infiltrant	Measuring dimension	Part A	Part B
ZCorp Z Bond 90	Volume	5	2
Smooth-On EpoxyAcast	Weight	10	3
Smooth-On EpoxyAmite	Volume	3	1
West Systems Epoxy	Volume	3	1

Once the samples were printed, color measurements were recorded. The next part of the section describes the color measurement of 3D printed samples.

4.2.1.2 Color Measurements

The color measurements were recorded in CIEL*a*b* color space using the Macbeth Color-Eye 7000 spectrophotometer shown in Figure 21. A spectrophotometer is an instrument designed to measure color in terms of reflectance across the spectrum. It was made available by the color measurement lab in the color science department at Rochester Institute of Technology.

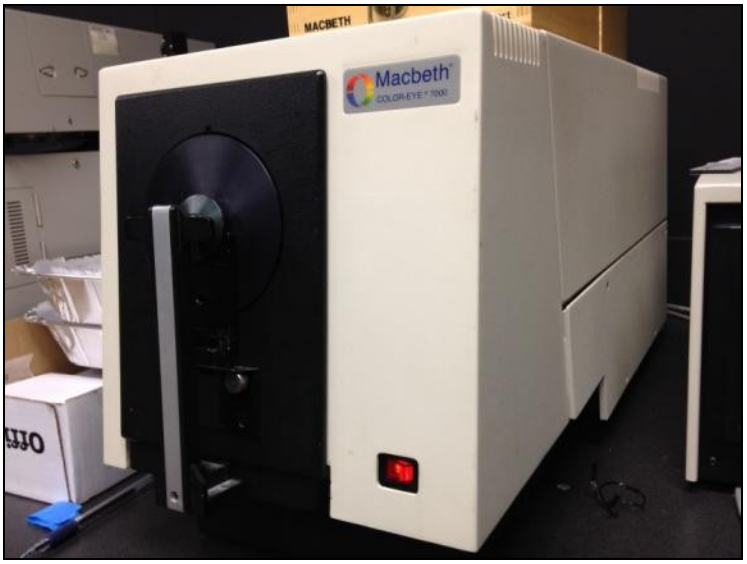

Figure 21: Color Eye 7000

The Color-Eye 70000 uses a Xenon flash that is triggered by a computer keyboard connected to an internal microprocessor via RS-232C communication port. The flash, after passing through a filter which approximates D65 lighting for a 10º observer, illuminates a diffusively reflective surface of the integrating sphere. In turn, the sample is illuminated. The reflected light from the sample then passes through an adjustable aperture on to a spectral analyzer consisting of a diffraction grating. The grating disperses the light into its spectral components. The detector array records the signal for further processing. The instrument also features a specular port for inclusion or exclusion of the specular component which is required for gloss measurement. The light from the wall of the integrating sphere serves as a reference for taking the measurements. The measurement in the form of reflectance of the sample across the spectrum can be recorded in an Excel spreadsheet using proprietary software. The reflectivity curve was plotted across the visual spectrum of wavelengths for each specimen at the specular and non-specular setting. A large aperture of 25mm diameter was chosen for experimental purposes to compensate for higher surface irregularities in 3D printing compared to the 2D printing process, and also to compensate for the inherent inconsistencies due to manual infiltration process.

OnColor software was used as the front end GUI for the spectrophotometer. The software allows the user to change the instrument settings and to do the instrument calibration. Each measurement is rendered on the screen with its delta with respect to a standard over the entire spectrum of wavelengths. A graphic of the same is also produced in a graph window. A screenshot of the software interface is shown in Figure 22 for illustration purposes. The screenshot below shows the screen after reflectivity measurements of a batch of samples was plotted across the visible spectrum.

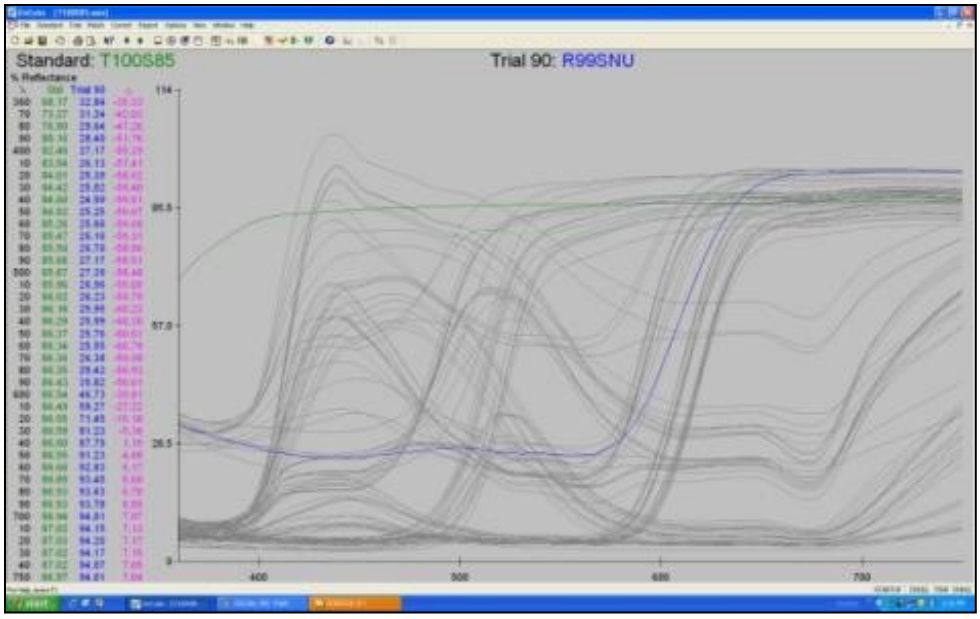

Figure 22 : OnColor Screen GUI

From the perspective of appearance, apart from the color value, one of the most important factors is gloss. Surfaces that demonstrate the phenomenon of mirror like reflections, which are known as specular reflections, are termed as glossy. Diffuse reflection gives rise to matte appearances. As part of the experiment, a qualitative assessment of gloss was also performed. All the 3D printed samples were classified into three categories, namely glossy, mixed and matte.

The glossy category consisted of samples exhibiting uniform glossy surface finishes. The ones without a glossy surface were categorized as matte samples. The samples that showed incomplete gloss coverage were categorized as mixed. This was a qualitative assessment, and the author is aware that further study would be required to draw statistically supported quantitative conclusions for gloss measurements.

4.2.2 Mechanical testing of infiltrated samples

One of the objectives of this research is to develop a response surface for color reproduction and mechanical behavior. Such a response surfaces would allow characterization of the trade-off behavior between color response and mechanical strength.

Following the ASTM D3039 standard for polymer composite matrix materials, the test specimens were generated accordingly. The length, width and thickness of the test coupons with uniform rectangular cross section were 205mm, 25mm and 4 mm respectively. These coupons were 3D printed using ZCorp Z510 at varying binder saturation, layer thickness and infiltrant. The effects of these process parameters and post processing method were studied by conducting a systematic factorial design experiment. According to the guidelines of ASTM D3039 and based on studies of mechanical testing (Lozo et al., 2008), the strain rate of 7mm/min was used to test elongation.

Tensile strength was determined using an Instron 4301 as seen in Figure 23. The equipment had a load cell with a capacity of 5KN.

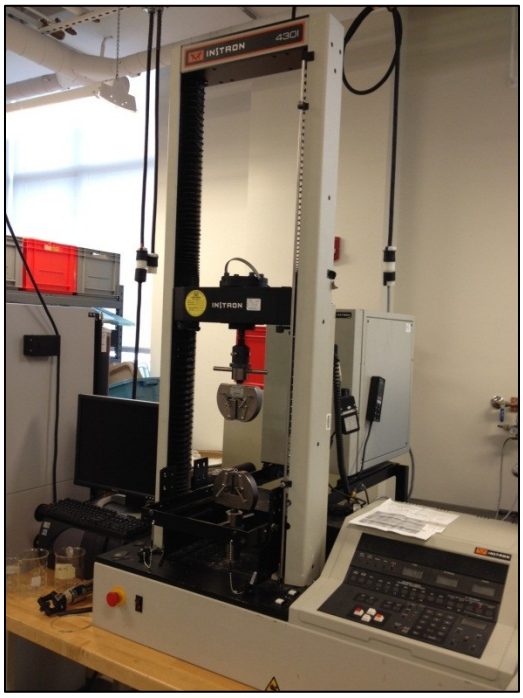

Figure 23: Instron 4301

BlueHill software was used to communicate with the Instron. As part of the setup, a test method was defined that specified parameters including strain rate. Other parameters specified during the test procedure included specimen dimensions, ambient temperature, and relative humidity. The sample was loaded in the Instron by adjusting the jaws to grip 25mm of the sample from both the ends. So, the effective gauge length of the sample was 155mm. The jaws of the gripper were tightened, and the unequal load at the end of the previous cycle and due to tightening of the jaws was balanced by clicking on the 'Load Balance' button on the GUI. After all the samples were measured, the software developed a report with all the tensile testing data and the stress strain curves. The measured tensile strength at break, which was measured in MPa, was used a metric of mechanical strength.

4.2.3 Wetting characteristics of 3D printed samples with various infiltrants

One of the factors that affect the strength, color reproduction, and gloss of 3D printed samples is the degree of infiltration. The contact angle largely determines the ease of penetration of the infiltrant for a given substrate. A first order experiment was conducted to measure the contact angle which determines the ease of infiltration for a given fluid. A Rame-Hart System was used to make direct contact angle measurements. It uses a goniometer and the DROPimage software to measure the contact angle. Initially, the measuring stage was leveled by a thumbscrew. The micro syringe assembly was then lowered until it appeared to one fourth of the level on the live camera screen. Then, focusing on the needle, the platform was adjusted till it appeared halfway on the screen. A two

micro liter drop of the first test epoxy was collected using the micro syringe assembly. The micro syringe was slowly lowered till the drop touched the pre cleaned glass substrate. Once the drop came in contact with the pre cleaned glass substrate, the micro syringe was slowly raised. Then the contact angle tool in the 'CA Tools' sub-menu was used to take the measurements. The baseline was setup by clicking snap with the delimiting lines set to the extreme points of the drop as seen in the on screen image. Finally, measurements were taken by clicking on the measure button on the GUI. In order to ensure that a correct measurement has been taken, the graphic of the angles measured was verified on the screen. Also, it was ensured that the contact angles at the left and the right extremes of the drop were almost the same. The above process is shown in Figure 24 which has been reproduced from the official product video.

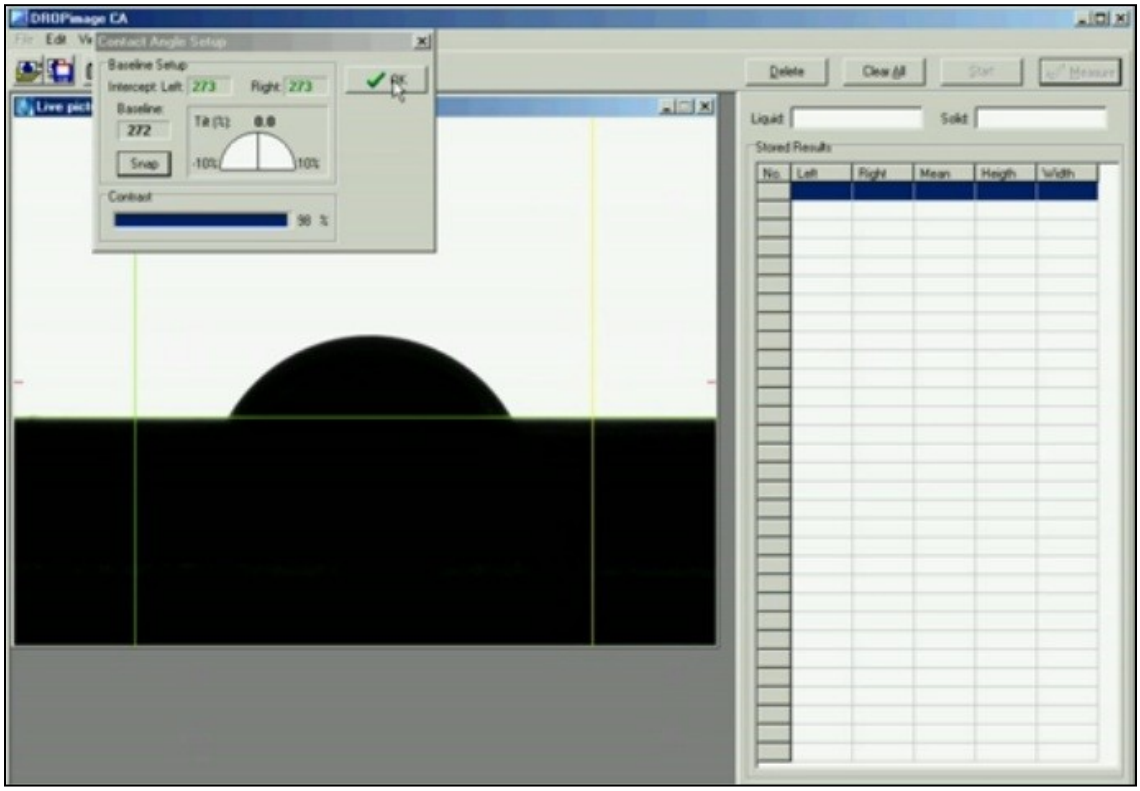

Figure 24: Contact angle measurement using DROPimage software (Ref: www.ramehart.com)

From the perspective of sample preparation, the part A and part B of the infiltrants were mixed in the recommended proportion as denoted in Table 2. After mixing the two parts together, the system was agitated for 1 minute to ensure thorough intermixing. The sample volume of the epoxy system was then loaded into the micro syringe and dropped on the measurement platform on the Rame-Hart system. Once deposited, the drop was allowed to stabilize the internal forces for a minute, and then the contact measurement was taken. Another measurement was taken after three minutes to determine the contact angle response as a function of time. The procedure was repeated for each of the four infiltrants. A sample measurement with EpoxyAmite is shown in Figure 25.

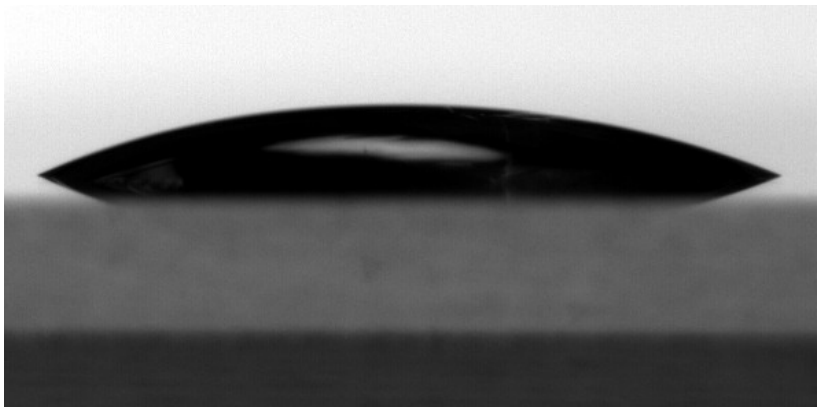

Figure 25: Image of a drop of EpoxyAmite on a glass substrate as seen in DROPimage software

4.2.4 Summary

After selecting the ZCorp 3D printing process to generate the experimental specimens, a full factorial experimental design was setup and samples were generated. To understand the effect of the control parameters on mechanical strength, a separate experiment was conducted by developing tensile test coupons. Lastly, first order estimate of wetting ability of each infiltrant under investigation was studied by measurement of contact angles. By conducting this exhaustive experimentation, it was possible to develop comprehensive data. The comprehensive nature of the experiment was a requirement to generate data for developing insights in the interaction effects. This data has been thoroughly analyzed and will be presented in the following section.

5 Analysis and Discussions

5.1 Color Measurements

5.1.1 Delta E

Delta E is the measure of perceived color difference. In the CIE L*a*b* system, it is given by the formula

$$\Delta E = \sqrt{[(\Delta L)^2 + (\Delta a)^2 + (\Delta b)^2]} \qquad \text{Equation 7}$$

The Delta E calculations are based on the uninfiltrated color response of sample printed at process parameters of layer thickness and shell binder saturation at levels recommended by Z Corporation. These delta E values were then plotted for each hue-saturation combination for varying process parameters and infiltration treatments. Figure 26 gives a visual illustration of the same.

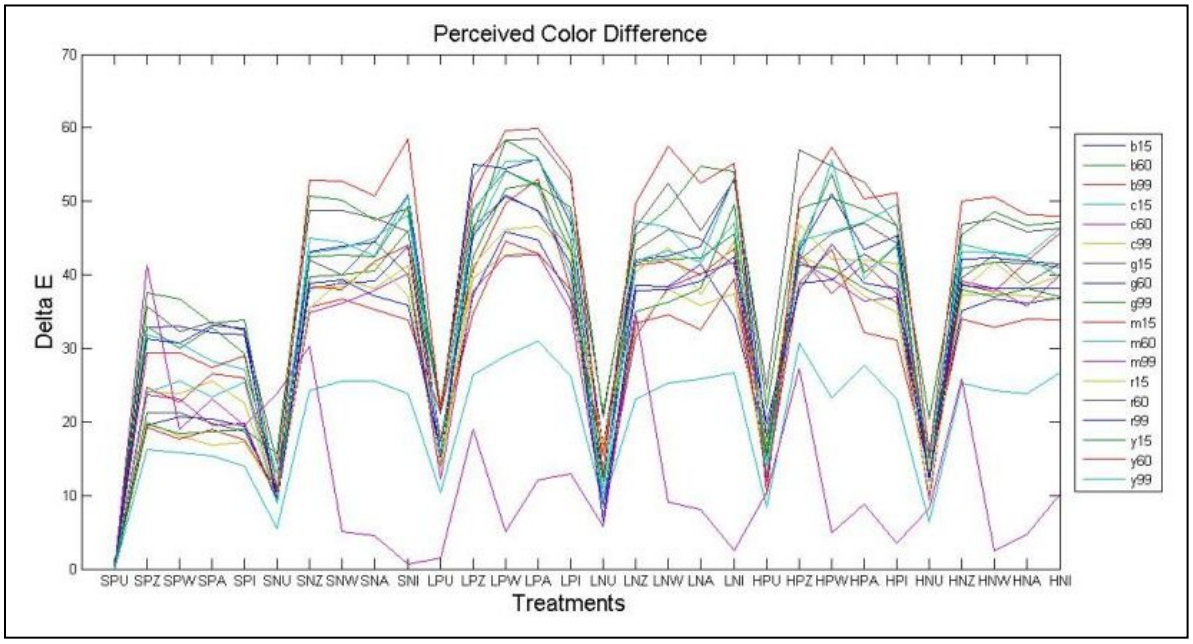

Figure 26: Delta E as a function of treatment combinations for each of the Hue-Saturation combination

It can be seen that the delta E values of uninfiltrated samples greatly differ from the delta E values of infiltrated samples. So the uninfiltrated samples were not included in the analysis. The ANOVA was used to understand the variation of delta E from the reference value of uninfiltrated samples. As the design has just one replicate, it should be noted that the error term is not comprised of pure error.

Table 3: ANOVA table for delta E with uninfiltrated samples as reference

ANOVA: (Delta E) non-color versus Hue, Coverage, ...

Factor	Type	Levels	Values
Hue	fixed	6	B, C, G, M, R, Y
Coverage	fixed	3	15, 60, 99
Layer Thickness	fixed	3	H, L, S
Binder Saturation	fixed	2	N, P
Infiltration	fixed	4	A, I, W, Z

Analysis of Variance for (Delta E) non-color

Source	DF	SS	MS	F	P
Hue	5	2849.73	569.95	60.32	0.000
Coverage	2	8360.81	4180.41	442.44	0.000
Layer Thickness	2	6661.61	3330.80	352.52	0.000
Binder Saturation	1	442.76	442.76	46.86	0.000
Infiltration	3	174.80	58.27	6.17	0.000
Hue*Coverage	10	830.34	83.03	8.79	0.000
Hue*Layer Thickness	10	320.88	32.09	3.40	0.000
Hue*Binder Saturation	5	266.73	53.35	5.65	0.000
Hue*Infiltration	15	123.66	8.24	0.87	0.596
Coverage*Layer Thickness	4	110.81	27.70	2.93	0.021
Coverage*Binder Saturation	2	219.83	109.92	11.63	0.000
Coverage*Infiltration	6	39.52	6.59	0.70	0.652
Layer Thickness*Binder Saturation	2	7083.65	3541.82	374.85	0.000
Layer Thickness*Infiltration	6	365.48	60.91	6.45	0.000
Binder Saturation*Infiltration	3	636.89	212.30	22.47	0.000
Error	355	3354.26	9.45		
Total	431	31841.77			

S = 3.07386 R-Sq = 89.47% R-Sq(adj) = 87.21%

Table 4: ANOVA of Delta E with higher order interactions

General Linear Model: (Delta E) non-color versus Hue, Coverage, ...

Factor	Type	Levels	Values
Hue	fixed	6	B, C, G, M, R, Y
Coverage	fixed	3	15, 60, 99
Layer Thickness	fixed	3	Hi, Int, Lo
Binder Saturation	fixed	2	N, P
Infiltration	fixed	5	A, I, U, W, Z

Analysis of Variance for (Delta E) non-color, using Adjusted SS for Tests

Source	DF	Seq SS	Adj SS	Adj MS	F	P
Hue	5	2588.22	2588.22	517.64	79.70	0.000
Coverage	2	7405.23	7405.23	3702.62	570.09	0.000
Layer Thickness	2	3932.30	3932.30	1966.15	302.73	0.000
Binder Saturation	1	63.07	63.07	63.07	9.71	0.003
Infiltration	4	46326.74	46326.74	11581.68	1783.22	0.000
Hue*Coverage	10	681.21	681.21	68.12	10.49	0.000
Hue*Layer Thickness	10	225.58	225.58	22.56	3.47	0.001
Hue*Binder Saturation	5	226.88	226.88	45.38	6.99	0.000
Hue*Infiltration	20	510.84	510.84	25.54	3.93	0.000
Coverage*Layer Thickness	4	29.30	29.30	7.32	1.13	0.349
Coverage*Binder Saturation	2	202.94	202.94	101.47	15.62	0.000
Coverage*Infiltration	8	1106.11	1106.11	138.26	21.29	0.000
Layer Thickness*Binder Saturation	2	5195.39	5195.39	2597.69	399.96	0.000
Layer Thickness*Infiltration	8	3626.06	3626.06	453.26	69.79	0.000
Binder Saturation*Infiltration	4	1608.30	1608.30	402.07	61.91	0.000
Hue*Coverage*Layer Thickness	20	380.85	380.85	19.04	2.93	0.000
Hue*Coverage*Binder Saturation	10	234.93	234.93	23.49	3.62	0.001
Hue*Coverage*Infiltration	40	289.26	289.26	7.23	1.11	0.336
Hue*Layer Thickness* Binder Saturation	10	136.12	136.12	13.61	2.10	0.034
Hue*Layer Thickness*Infiltration	40	453.69	453.69	11.34	1.75	0.017
Hue*Binder Saturation*Infiltration	20	201.56	201.56	10.08	1.55	0.087
Coverage*Layer Thickness* Binder Saturation	4	168.79	168.79	42.20	6.50	0.000
Coverage*Layer Thickness* Infiltration	16	447.78	447.78	27.99	4.31	0.000
Coverage*Binder Saturation* Infiltration	8	101.68	101.68	12.71	1.96	0.063
Layer Thickness*Binder Saturation* Infiltration	8	2524.01	2524.01	315.50	48.58	0.000
Hue*Coverage*Layer Thickness* Binder Saturation	20	350.00	350.00	17.50	2.69	0.001
Hue*Coverage*Layer Thickness* Infiltration	80	374.36	374.36	4.68	0.72	0.928
Hue*Coverage*Binder Saturation* Infiltration	40	186.34	186.34	4.66	0.72	0.876
Hue*Layer Thickness* Binder Saturation*Infiltration	40	328.58	328.58	8.21	1.26	0.185
Coverage*Layer Thickness* Binder Saturation*Infiltration	16	357.83	357.83	22.36	3.44	0.000
Error	80	519.59	519.59	6.49		
Total	539	80783.52				

S = 2.54849 R-Sq = 99.36% R-Sq(adj) = 95.67%

Based on the ANOVA presented in Table 3, it is observed that hue, coverage and layer thickness account for most of the variation, along with the interaction between layer thickness and binder saturation. Table 4 presents the analysis with all higher order interactions included.

In Figure 27, it should be noted that the absolute values of delta E are misleading because they have been referenced from uninfiltrated samples. Further, looking at the main effects plot, a large difference in the delta E levels of uninfiltrated samples in comparison to the infiltrated samples can be observed. However, there is very little variation within the infiltrated samples. Thus, the process of infiltration is significant; however the choice of infiltrant is not a significant factor in determining delta E.

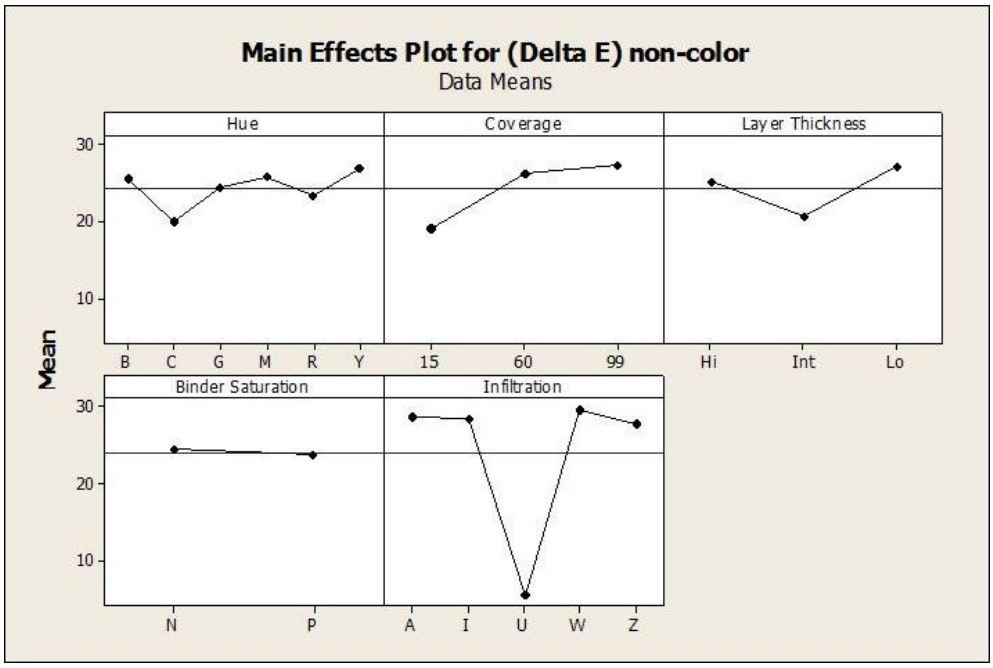

Figure 27: Main Effects plot of Delta E

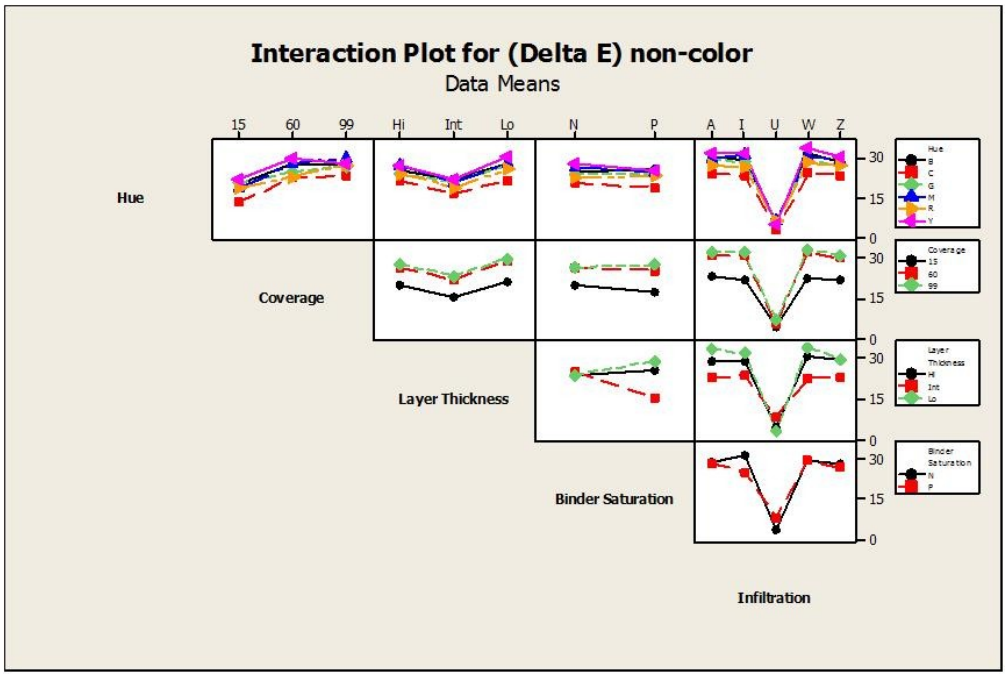

Figure 28: Interaction effects of delta E

From the interaction effects plot presented in Figure 28, the following observations can be made:

- The samples with 15% coverage have lower delta E values.
- Low binder saturation leads to loss of sensitivity of delta E to changes in layer thickness

Residual Analysis

The normal probability plot seen in Figure 29 satisfies the normality assumption inherent with the ANOVA. Further, the histogram in Figure 30 follows the classic bell curve which reinforces the assumption of normality of the data.

The residuals show a distinct trend, however given the batch processing constrains on printing and infiltration in the experiment, it was not possible to randomize the runs.

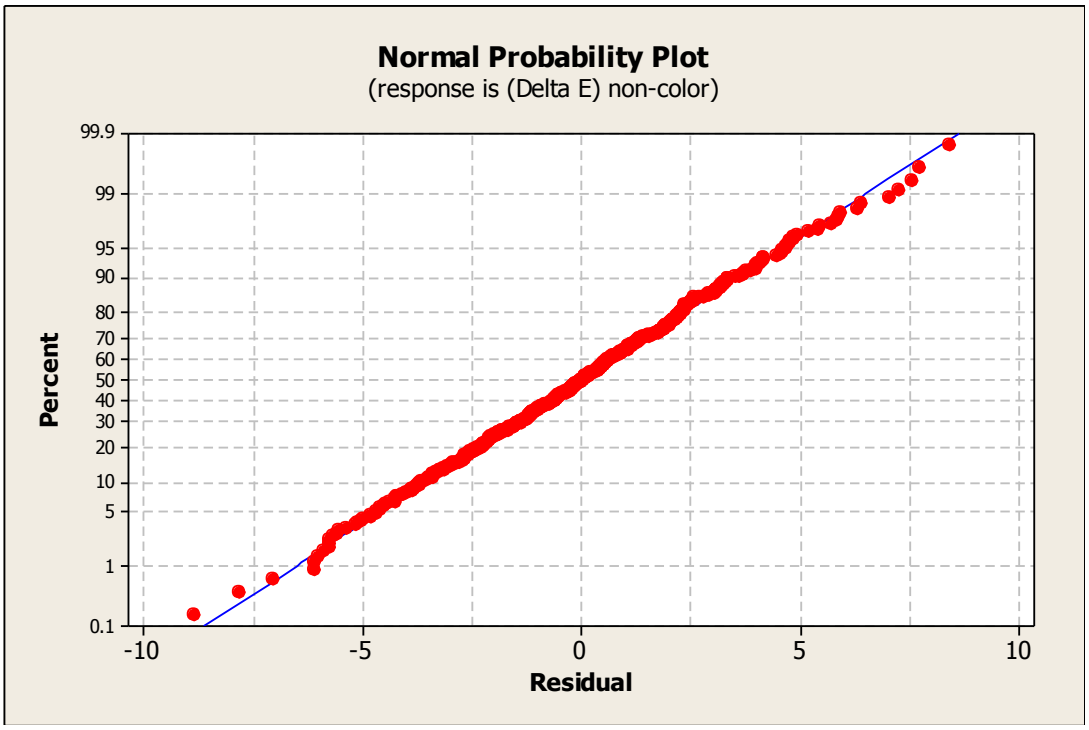

Figure 29: Normal Probability Plot of Delta E

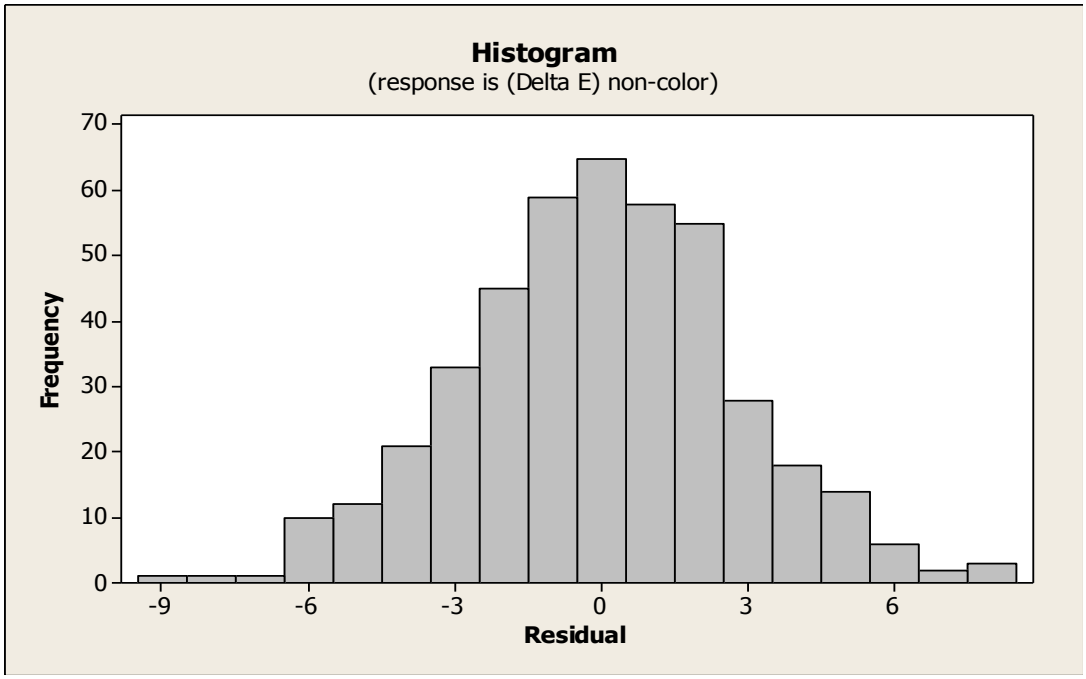

Figure 30: Histogram of Delta E

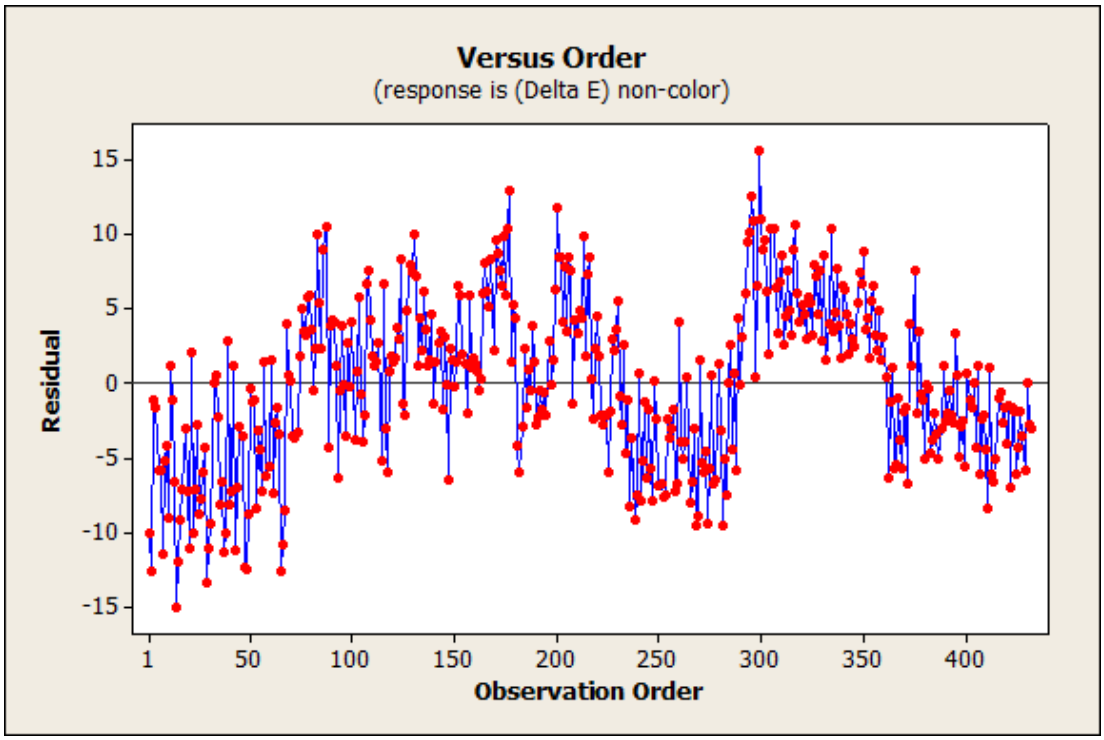

Figure 31: Trend seen in residuals versus observation order

5.1.2 Lightness, Chroma and Hue

Lightness, Chroma and Hue are the individual components of color in the CIEL*C*H* color space. Similar to Delta E, ANOVA was conducted on lightness, chroma and hue. The following section initially delineates the main effect and interaction effect plots of lightness, chroma and hue in Figure 32, Figure 33, Figure 34, Figure 35, Figure 36 and Figure 37.

Then, important observations regarding these response variables are noted and inferences will be presented in the light of previous research findings in the area.

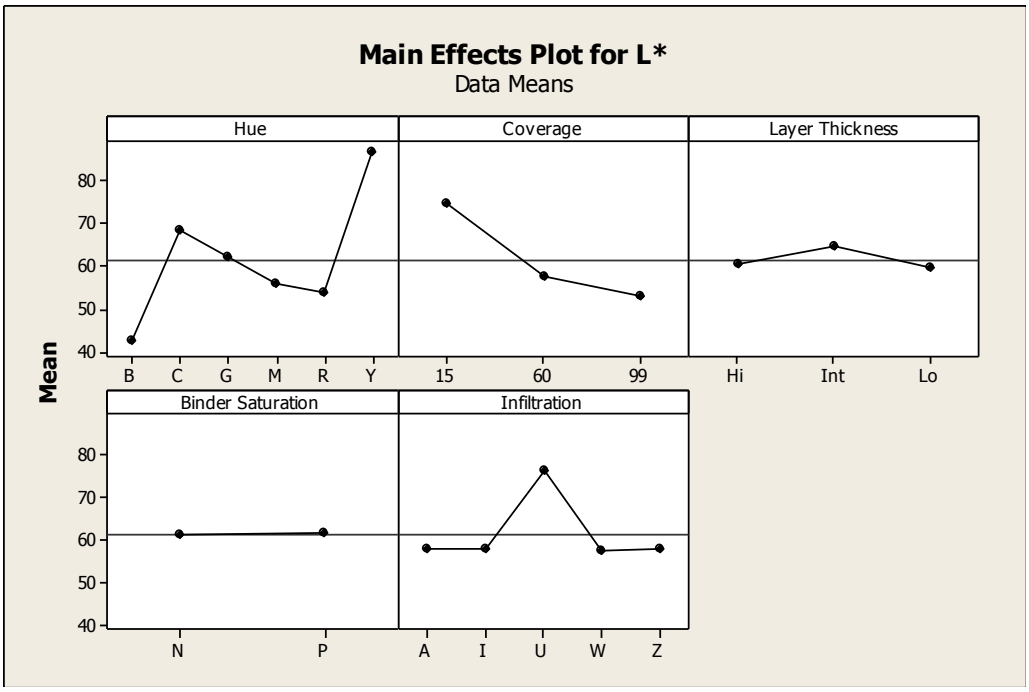

Figure 32: Main effects plot for L*

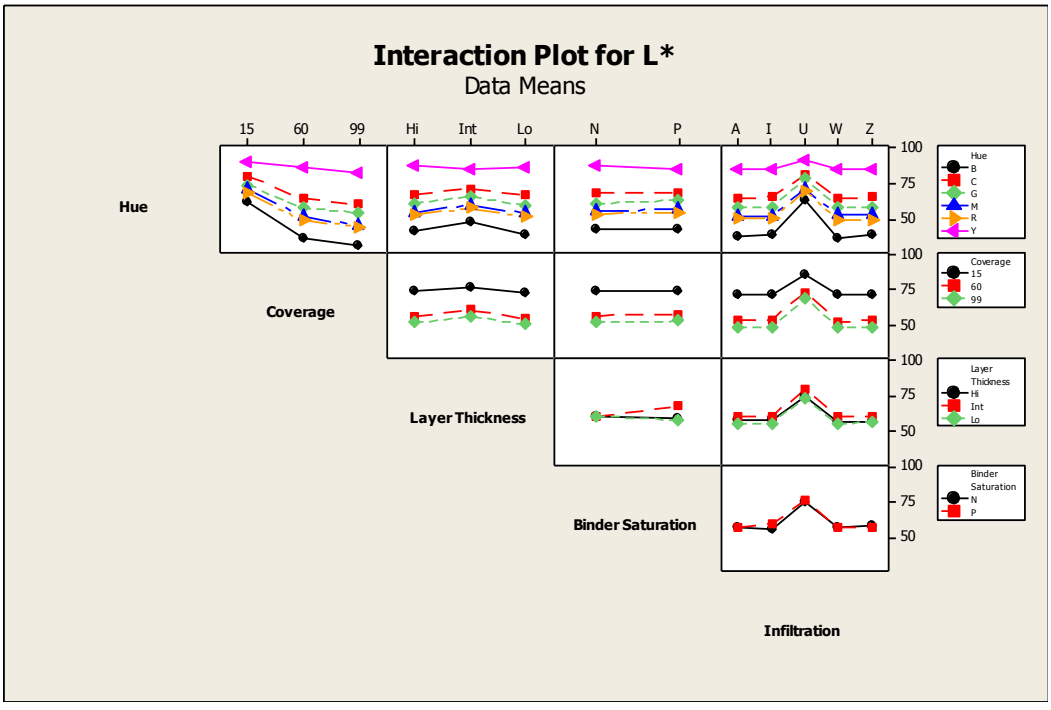

Figure 33: Interaction effects plot for L*

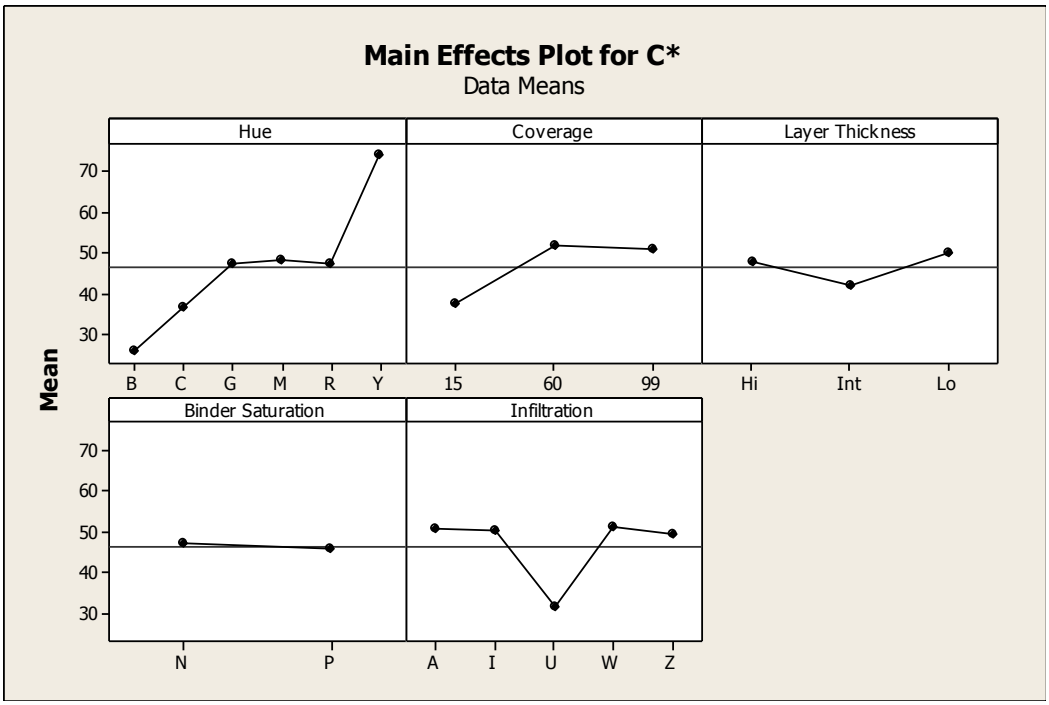

Figure 34: Main effects plot for C*

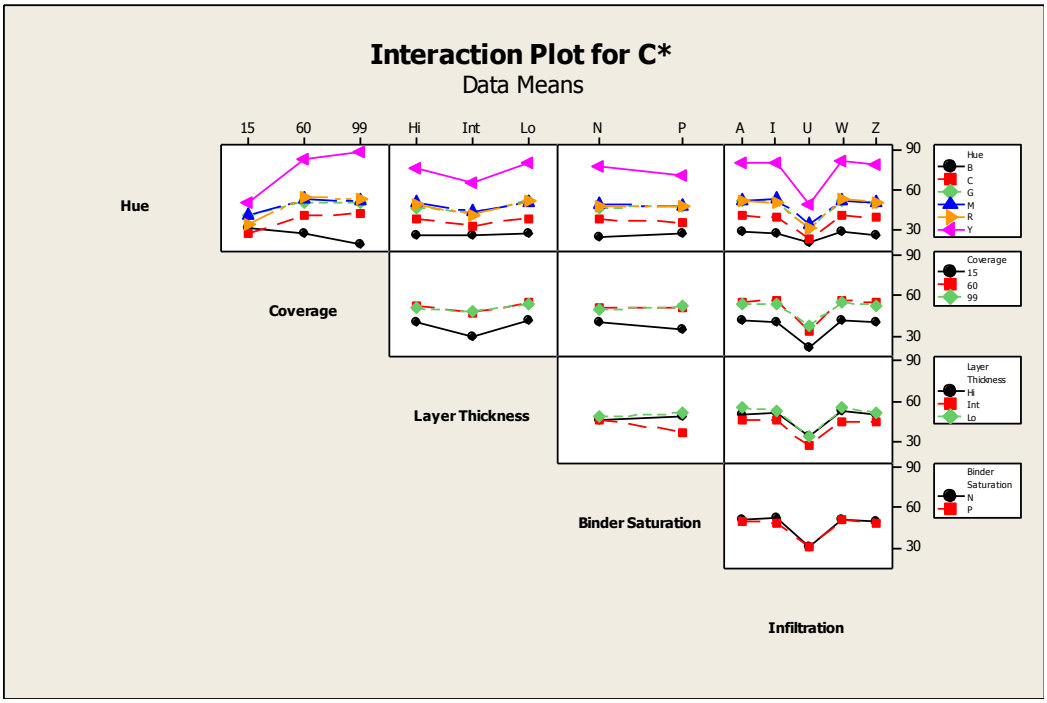

Figure 35: Interaction effects plot for C*

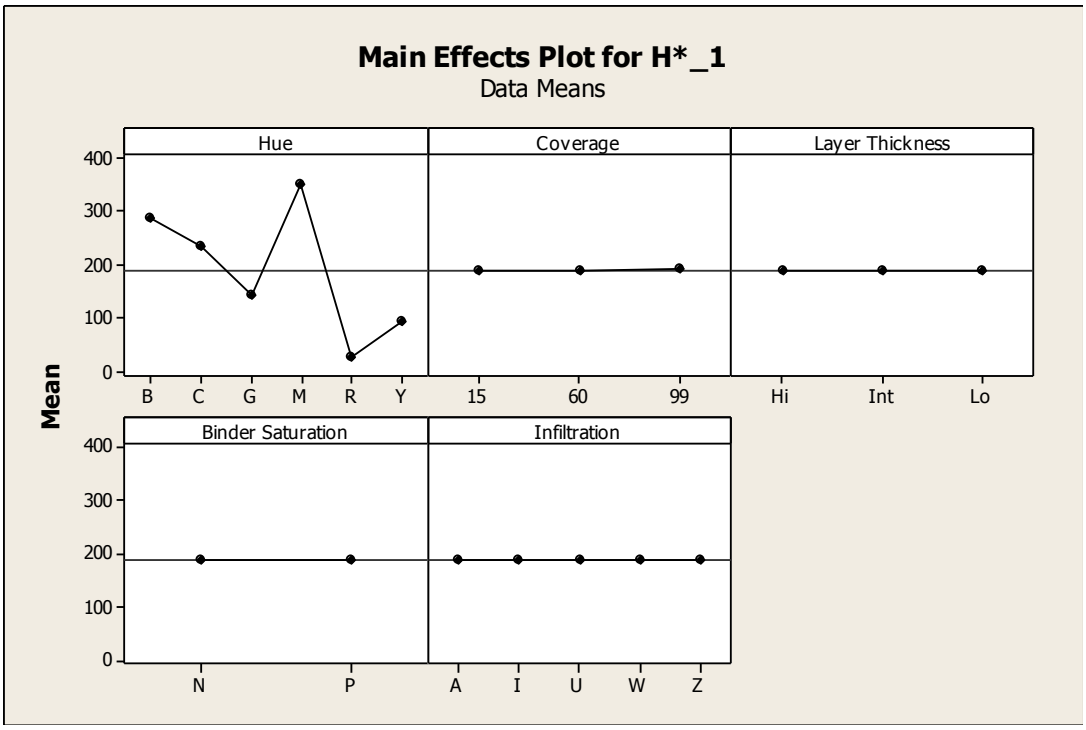

Figure 36: Main effects plot for H*

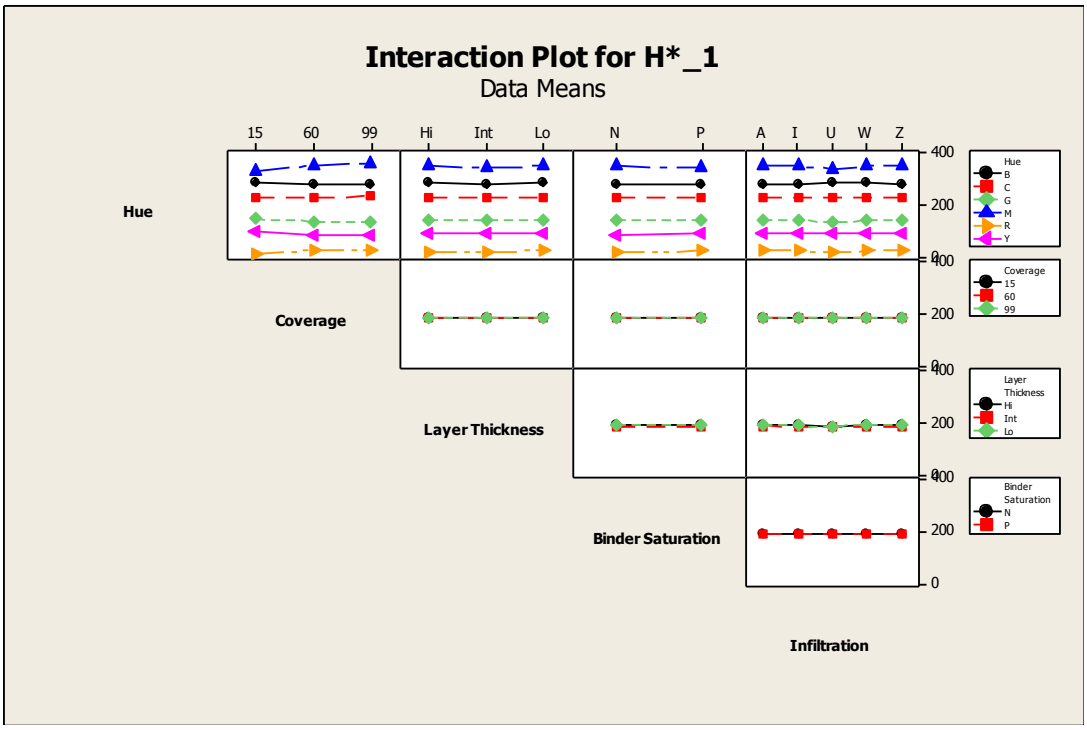

Figure 37: Interaction effects plot for H*

Observations on response of Lightness (L*)

- L* values are higher at the recommended setting of high binder saturation and medium Layer thickness compared to other combinations of process parameters
- L* values are higher for uninfiltrated samples. This finding corroborates exactly with the previous research on color measurement in 3D printed structures (Stanic et al., 2008).

Observations on response of Chroma (C*)

- C* values are lower at recommended setting of high binder saturation and intermediate layer thickness
- Also, C* values are lower for uninfiltrated samples. This finding corroborates exactly with the previous research on color measurement in 3D printed structures (Stanic et al., 2008).

Observations on response of Hue (H*)

- Observations of H* do not show any particular trend or pattern, which indicates that the printing process is under control and that there is not erratic variation underlying the other observations.

5.2 Mechanical Performance Measurements

Initially, main effects and interaction effects were explored as seen in Figure 38 and Figure 39. It is evident that uninfiltrated samples show very low tensile strength compared to the infiltrated ones. It should be noted that measuring uninfiltrated samples with ASTMD3039 standards is not advisable because their material structure is not that of a polymer composite matrix. Hence, the data set was filtered to include only the infiltrated samples

The results of the mechanical testing were analyzed using ANOVA. It can be seen from Table 5that infiltration, layer thickness and the interaction of layer thickness and binder saturation are statistically significant effects at 95% confidence interval. The adjusted R^2 value of the model is 79.68%, which indicates that the model accounts for a high degree of variation in tensile strength with changes in process parameters.

Table 5: ANOVA for tensile strength as a response of infiltration, layer thickness and binder saturation

ANOVA: Tensile Stre versus Infiltration, Layer Thickn, Binder Satur

Factor	Type	Levels	Values
Infiltration	fixed	4	A, I, W, Z
Layer Thickness	fixed	3	Hi, Int, Lo
Binder Saturation	fixed	2	N, P

Analysis of Variance for Tensile Strength at Failure MPa

Source	DF	SS	MS	F	P
Infiltration	3	32.616	10.872	7.87	0.017
Layer Thickness	2	38.768	19.384	14.04	0.005
Binder Saturation	1	3.034	3.034	2.20	0.189
Infiltration*Layer Thickness	6	14.533	2.422	1.75	0.256
Infiltration*Binder Saturation	3	4.743	1.581	1.15	0.404
Layer Thickness*Binder Saturation	2	54.330	27.165	19.67	0.002
Error	6	8.285	1.381		
Total	23	156.309			

S = 1.17508 R-Sq = 94.70% R-Sq(adj) = 79.68%

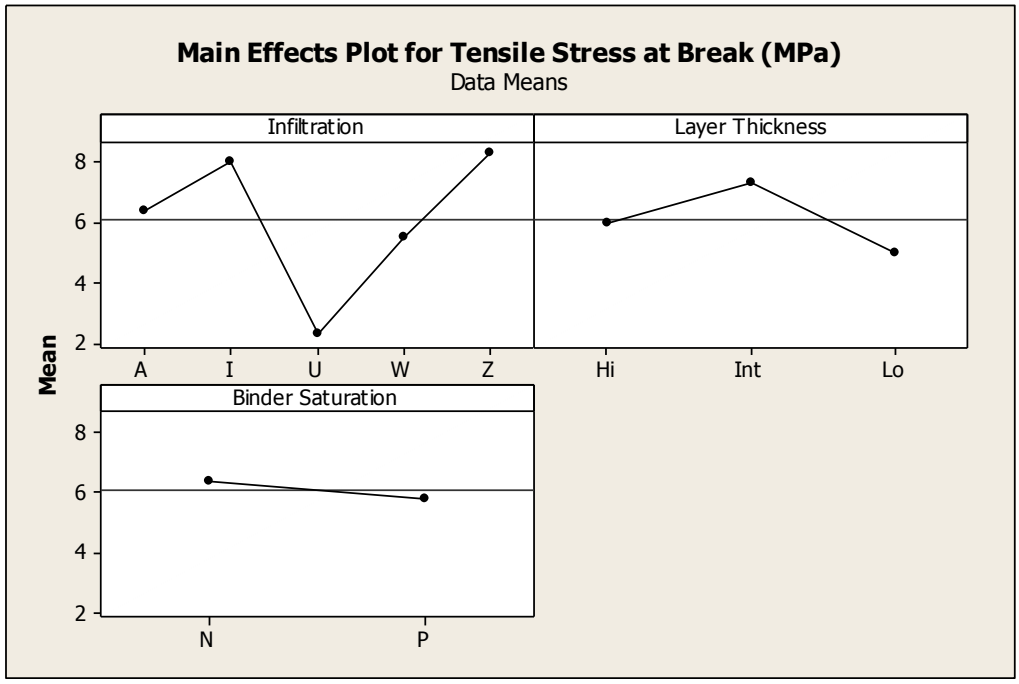

Figure 38: Main effects plot of tensile strength at break

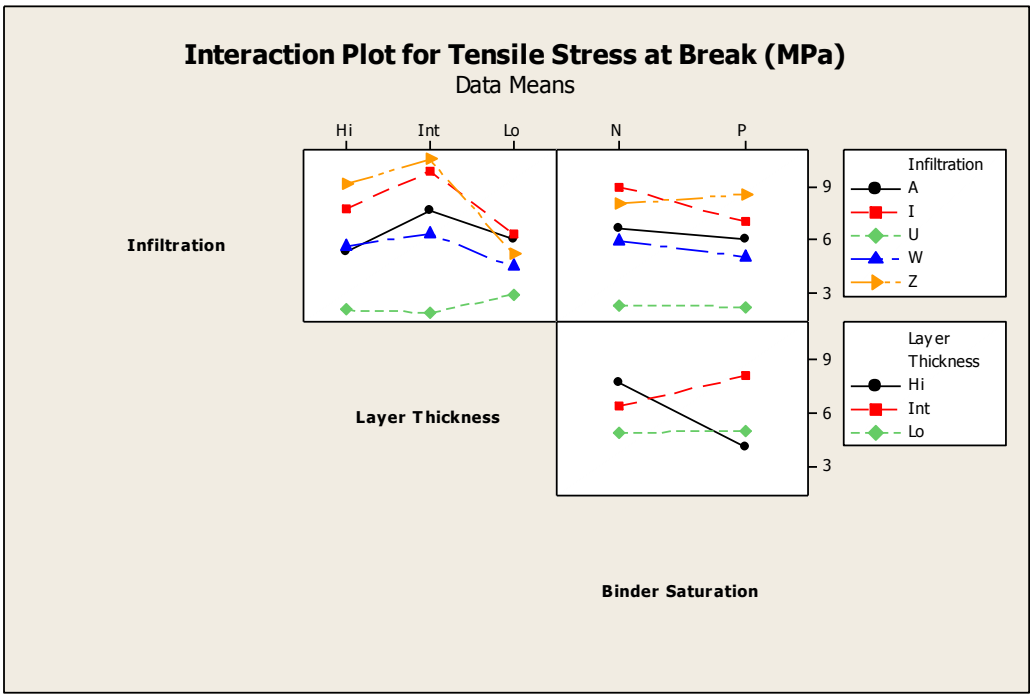

Figure 39: Interaction effects plot of tensile strength at Break

Inferences

- The recommendation of combination of layer thickness of 0.100mm and a binder saturation of 100% produces the highest mechanical strength.
- The combination of layer thickness of 0.114mm and a binder saturation of 85% produces nearly equal mechanical strength.
- It is evident that the uninfiltrated samples have very low tensile strength compared to the infiltrated samples.
- Among the infiltrants, ZMax 90 and EpoxyAmite produce samples with much better tensile strength than the EpoxyAcast and West Systems epoxy.

Validation check

In order to better understand the reason behind the apparent difference in tensile strength of samples, a simple infiltration test was conducted. A cross section of each test coupon was dipped in dye based colored solution. As seen in Figure 40, the colored solution was absorbed by most of the samples, indicating incomplete infiltration. This implies that the mechanical strength recorded on these parts has been below the true mechanical strength of completely infiltrated parts.

Two process parameter combinations do not show significant absorption of colored solution, indicating that they are completely infiltrated. These process combinations correspond to samples with the highest mechanical strength and are:

Layer thickness = 0.100mm and binder saturation = 100%
Layer thickness = 0.114mm and binder saturation = 85%

It should be noted that the infiltration conditions on each of these samples were identical. This suggests that only certain process combinations enhance the ease of infiltration of 3D printed parts. These process combinations in return yield samples with the highest tensile strength.

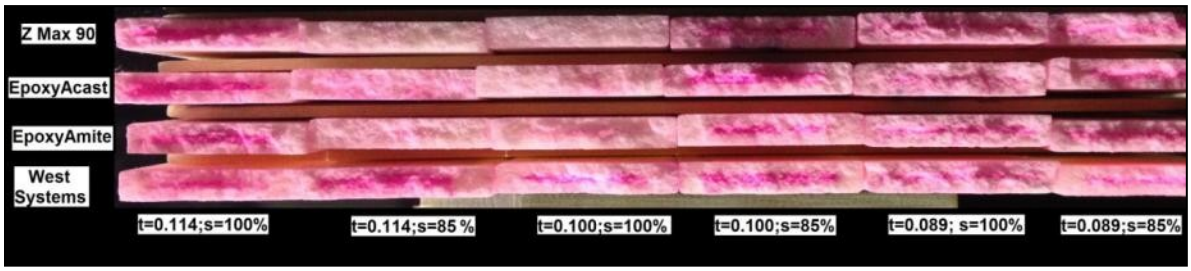

Figure 40: Varying infiltration depth in at varying levels of layer thickness and binder saturation

This experiment has been the first one to explore the tensile test of 3D printed infiltrated test coupons. The observations from previous research in characterization of mechanical strength as a response to layer thickness and binder saturation in uninfiltrated samples (Vaezi & Chua, 2011) do not extend to infiltrated samples. This suggests that the mechanical strength of infiltrated samples arises from attributes different than those in uninfiltrated samples.

5.3 Gloss Measurement

5.3.1 Visual Inspection

Surface appearance is measured in terms of gloss. Initially a visual inspection was carried out to gain an understanding of the gloss mechanisms. Table 6 shows two different surface appearances under standard magnification and at magnification of 50x captured using the Hirox Microscope in the Brinkman Lab.

Table 6 : Gloss measurement of various samples

Sample type	Macro Image	Micro Image
Matte	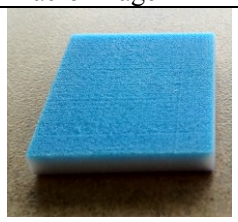	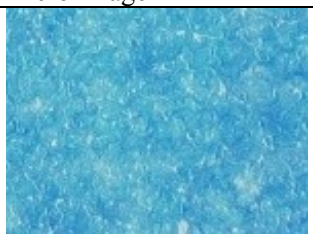
Glossy		

Observations and inferences

The image above depicts the differences between glossy surfaces and matte surfaces. In the top image, the left hand side sample is matte while the right hand side sample is glossy. On observing under a microscope, it can be seen that for the matte image there is a random highly dense areas of highlight in the image. These highlighted areas are sites from which incident light gets scattered in all directions leading to a matte appearance. The glossy sample reveals no such areas, and the surface is smooth without irregularities. This leads to specular reflection that renders a glossy appearance.

5.3.2 Statistical Analysis

ANOVA was conducted to better understand the effect of the control parameters on gloss as a categorical response. From Table 7, it can be seen that the model describes gloss as a response of hue, coverage, layer thickness, binder saturation and infiltration.

Table 7: ANOVA for gloss as a response to hue, coverage, layer thickness, binder saturation and infiltration

General Linear Model: Gloss versus Layer Thickn, Binder Satur, ...

```
Factor             Type   Levels  Values
Layer Thickness    fixed       3  Hi, Int, Lo
Binder Saturation  fixed       2  N, P
Infiltrant         fixed       5  A, I, U, W, Z


Analysis of Variance for Gloss, using Adjusted SS for Tests

Source                         DF    Seq SS   Adj SS   Adj MS       F      P
Layer Thickness                 2   42.0111  42.0111  21.0056  139.74  0.000
Binder Saturation               1   12.1500  12.1500  12.1500   80.83  0.000
Infiltrant                      4   46.8963  46.8963  11.7241   77.99  0.000
Layer Thickness*Binder Sat      2   14.0778  14.0778   7.0389   46.83  0.000
Layer Thickness*Infiltrant      8   12.0259  12.0259   1.5032   10.00  0.000
Binder Saturation*Infiltrant    4    5.1556   5.1556   1.2889    8.57  0.000
Error                         518   77.8667  77.8667   0.1503
Total                         539  210.1833

S = 0.387713   R-Sq = 62.95%   R-Sq(adj) = 61.45%
```

The adjusted R^2 value of the model is 61.45%, which indicates that the model accounts for a high degree of variation in gloss with change in layer thickness, binder saturation, and infiltration. The residual analysis was conducted using a normal probability plot of the residuals and histogram, depicted in Figure 41 and Figure 42 respectively which verified the normality assumptions.

Further, the main and interaction effects plots have been plotted as seen in Figure 43 and Figure 44.

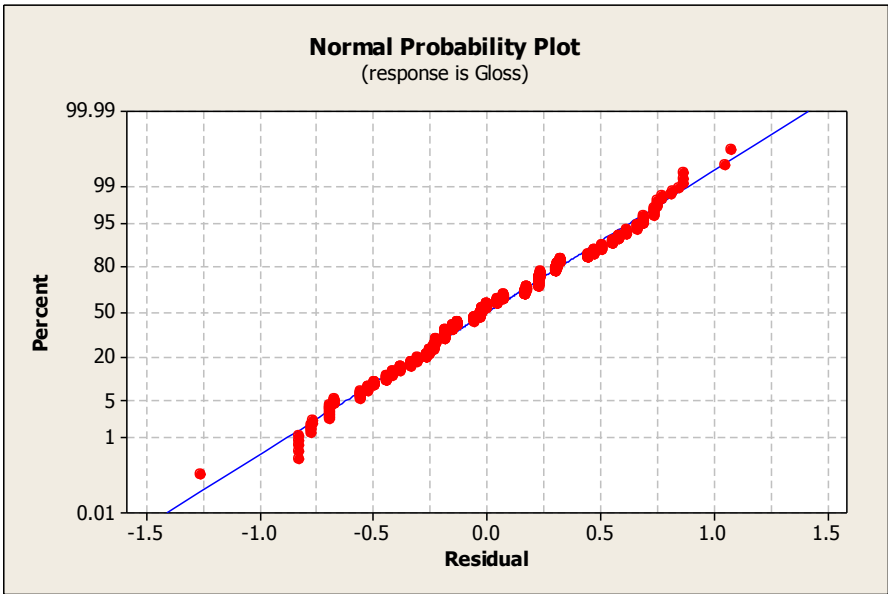

Figure 41: Normal probability plot of gloss as a response of layer thickness, binder saturation and infiltration

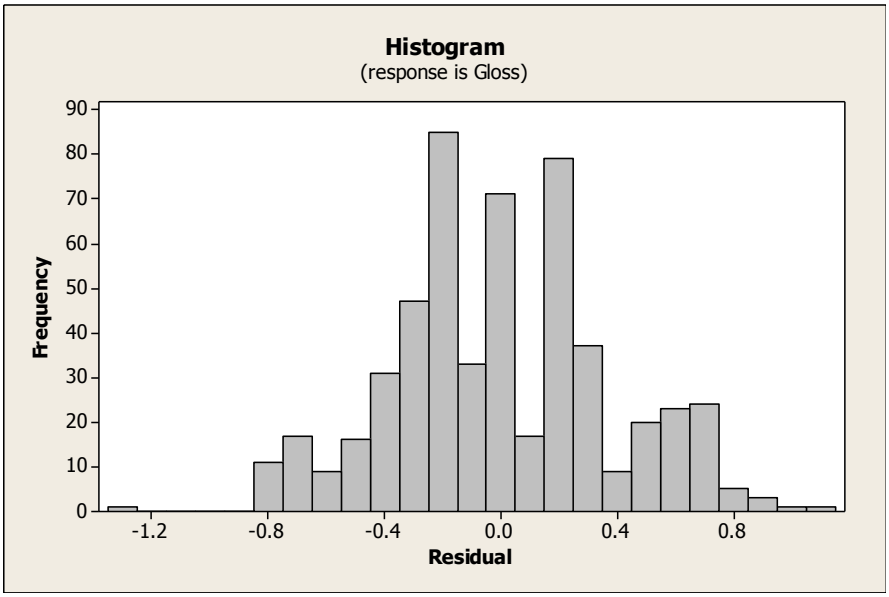

Figure 42: Histogram of gloss as a response of layer thickness, binder saturation and infiltration

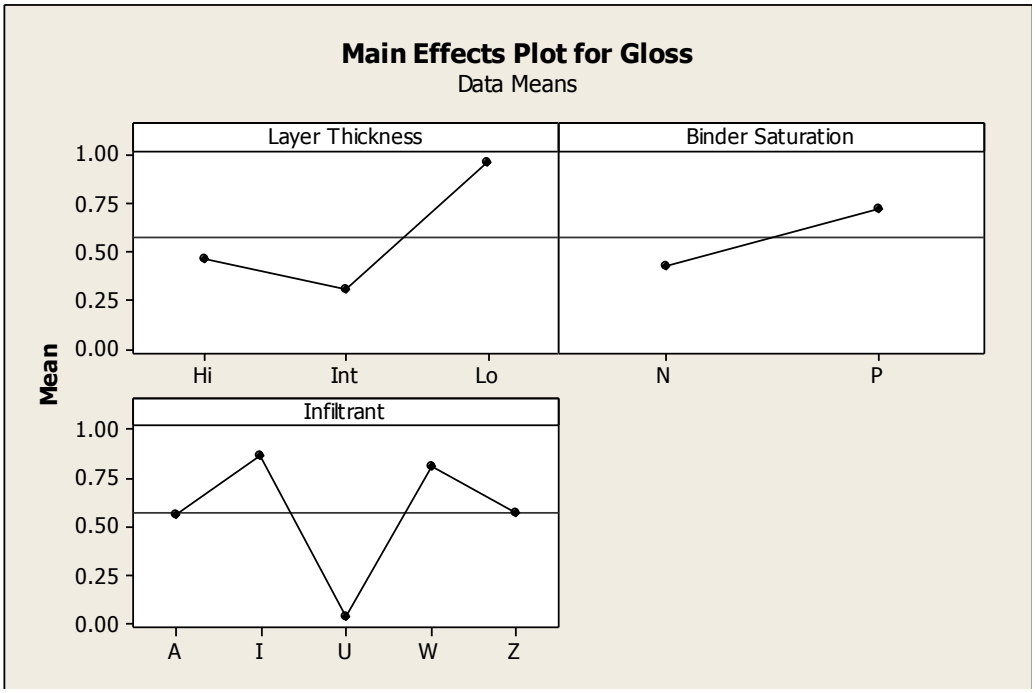

Figure 43: Main effects plot for gloss

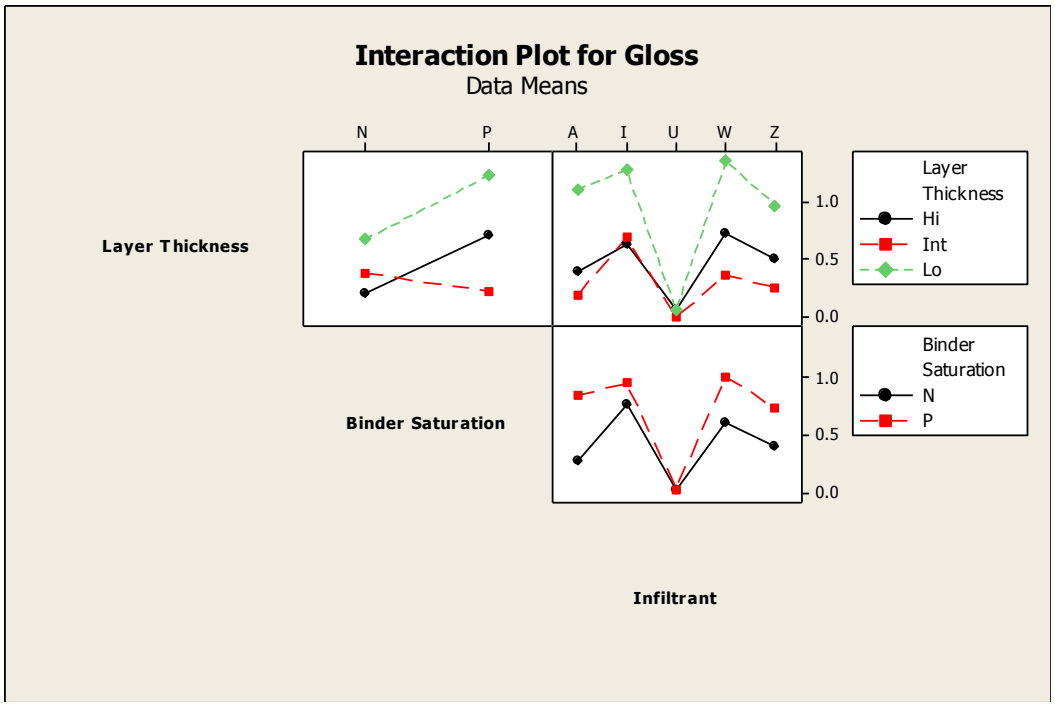

Figure 44: Interaction effects plot for gloss

From the ANOVA, it can be seen that all factors and their interactions are significant. It can be seen that any infiltration significantly increases the glossy appearance of the part. Further, EpoxyAmite and West Systems Epoxy yield a more glossy appearance compared to Z Max 90 and EpoxyAcast.

Also, there is a sharp increase in the glossy appearance with a decrease in layer thickness from 100 microns to 89 microns. It is worth noting that there is small increase in the gloss with increase in the layer thickness beyond 100 microns as well. Further, there is a distinct decrease in glossy appearance with reduced shell saturation.

6 Conclusions

The effect of layer thickness and binder saturation in 3D inkjet printing on color reproduction was studied using a factorial experiment. Layer thickness was found to be a significant factor which accounted for a large degree of variation in color response. The effect of infiltration on color reproduction was also studied. In this experiment, the interaction effect between layer thickness and binder saturation was also found to be significant. Low binder saturation causes loss of sensitivity of delta E to change in layer thickness. It was further found that the recommended combination of layer thickness and binder saturation is not favorable for vivid color reproduction.

The mechanical strength of 3D parts printed at different process parameters subjected to post processing with different infiltrant was also studied. It was observed that the recommended process parameters result in parts that are easier to infiltrate, which in turn leads to higher mechanical strength. Further, it was found that the combination of 0.114mm layer thickness and 85% binder saturation resulted in parts with comparable mechanical strength. Also, the use of ZCorp recommended Z Max 90 infiltrant results in parts with the highest tensile strength. The EpoxyAmite infiltrant also provides mechanical performance comparable with ZCorp.

Based on these two findings, it is evident that one single set of process combination does not produce the best color results and mechanical performance at the same time. Tradeoffs were explored. It was identified that for the most vivid color reproduction, infiltration is required, but the choice of infiltrant is not significant. Further, for vivid color reproduction, process parameters should not be set at a combination of 0.100mm layer thickness and 100% binder saturation. For good mechanical performance, two process combinations are suitable. First is the recommended combination of 0.100mm layer thickness and 100% binder saturation, while the second is 0.114mm layer thickness and 85% binder saturation. Also, ZMax 90 and EpoxyAmite are suitable for high strength parts. A real world use case scenario would require a certain degree of mechanical strength with a certain level of color vibrancy. In such a case, the process parameters and infiltrants need to be carefully adjusted to achieve an optimum balance between color vibrancy and mechanical strength.

7 Future Work

The research study is limited to achieving selective coloring at only the outermost layer. The applications of rapid prototyping would grow exponentially if selective coloring can be achieved throughout the object. To date, there exists no commercial process to achieve this. Such a process development activity would require integrated efforts of cross functional teams of color scientists and engineers with expertise in mechanical design and control systems.

Another research area in this field is the testing of different infiltrants and developing an infiltrant independent parametric modeling of 3D prints to achieve a balance of mechanical strength and color reproduction. The research has explored the contact angle in an attempt to correlate physical properties of the infiltrant to the color reproduction that they achieve in 3D printed parts. The effect of other physical properties including viscosity, optical density and volatility of infiltrant on color reproduction are the areas that warrant further research.

ICC color profiling is a technique to study the background or the substrate color, and then suitably adjust the actual colors printed so that the visual perception becomes independent of background color. The technique holds promise for the development of full colored 3D printed structures and is another potential field of future study.

Low binder saturation makes the color response less sensitive to changes in layer thickness. Further, binder saturation does not appear to contribute much towards mechanical strength of the part. This observation opens up possibilities of maintaining color reproduction within a process capable of dynamically varying layer thickness, and to match the contours of the part geometry towards optimized build times.

8 References

Berns, R. S. (2000). Billmeyer and Saltzman's principles of color technology: Wiley New York.

Bynum, D. K. (1992). Automated manufacturing system using thin sections: Google Patents.

Carr, W. W., Sarma, D. S., Cook, F. L., Shi, S., Wang, L., & Pfromm, P. H. (1998). Studies on toners for textile xerography. Journal of Electrostatics, 43(4), 249-266. doi: 10.1016/S0304-3886(98)00007-2

Chua, C. K., Leong, K. F., & Lim, C. S. (2010). Rapid prototyping: principles and applications: World Scientific Pub Co Inc.

Cormier, D., Taylor, J., Unnanon, K., Kulkarni, P., & West, H. (2000). Experiments In Layered Electro-Photographic Printing. 2000 Solid Freeform Fabrication Proceedings, 7-9.

Cormier, D., Taylor, J., & West, H. (2002). An investigation of selective coloring with 3-D laser printing. Journal of Manufacturing Processes, 4(2), 148-152. doi: 10.1016/s1526-6125(02)70141-2

Grenda, E. P. (1996). Apparatus and method of fabricating 3-dimensional objects by means of electrophotography, ionography or a similar process: EP Patent 0,702,623.

Hopkinson, N., & Dickens, P. (2001). Rapid prototyping for direct manufacture. Rapid Prototyping Journal, 7(4), 197-202.

Hunter, R. S., & Harold, R. W. (1987). The measurement of appearance: Wiley-Interscience.

Im, Y. G., Chung, S. I., Son, J. H., Jung, Y. D., Jo, J. G., & Jeong, H. D. (2002). Functional prototype development: inner visible multi-color prototype fabrication process using stereo lithography. Journal of materials processing technology, 130, 372-377.

Jones, J., Wimpenny, D. I., Gibbons, G., & Sutcliffe, C. (2010). Additive manufacturing by electrophotography: Challenges and successes. Paper presented at the International Conference on Digital Printing Technologies.

Jones, J. B., Gibbons, G. J., & Wimpenny, D. I. (2011). Transfer methods toward additive manufacturing by electrophotography.

Kumar, A. V. (2000). Solid freeform fabrication using power deposition: Google Patents.

Kumar, A. V., & Dutta, A. (2003). Investigation of an electrophotography based rapid prototyping technology. Rapid Prototyping Journal, 9(2), 95-103.

Lozo, B., Stanić, M., Jamnicki, S., Poljaček, S. M., & Muck, T. (2008). Three-Dimensional Ink Jet Prints—Impact of Infiltrants. Journal of Imaging Science and Technology, 52, 051004.

Mahabadi, H. K., & Alexandru, L. (1985). Toner compositions containing thermotropic liquid crystalline polymers: Google Patents.

Ming, L. W., & Gibson, I. (1999). Possibility of colouring SLS prototypes using the ink-jet method. Rapid Prototyping Journal, 5(4), 152-154.

Noorani, R., & Knovel. (2006). Rapid prototyping: Wiley.

Parraman, C., Walters, P., Reid, B., & Huson, D. (2008). Specifying colour and maintaining colour accuracy for 3D printing. Proceedings of Electronic Imaging, Society for Imaging Science and Technology/Society of Photographic Instrumentation Engineers, San Jose, CA, USA, 26-31 January 2008.

Pugh, S. (1981, 1981). Concept selection: A method that works. Paper presented at the International Conference on Engineering Design, Rome.

Rees, M. (1998). Color: completing rapid prototyping as a mature communications media. Prototyping Technology International, May.

Sachs, E., Cima, M., Cornie, J., Brancazio, D., Bredt, J., Curodeau, A., . . . Lee, J. (1993). Three-dimensional printing: the physics and implications of additive manufacturing. CIRP Annals-Manufacturing Technology, 42(1), 257-260.

Schein, L. B. (1999). Recent advances in our understanding of toner charging. Journal of electrostatics, 46(1), 29-36.

Stanic, M., Lozo, B., Muck, T., Jamnicki, S., & Kulcar, R. (2008). Color Measurements of Three-Dimensional Ink-Jet Prints (pp. 623-626). Pittsburgh, Pennsylvania: NIP24: International Conference on Digital Printing Technologies and Digital Fabrication 2008.

Stanic, M., Lozo, B., & Svetec, D. G. (2012). Colorimetric properties and stability of 3D prints. Rapid Prototyping Journal, 18(2), 120-128.

Stanić, M., Lozo, B., & Walters, P. J. (2010). Reproduction in Three-Dimensional Ink Jet Printing. Journal of Imaging Science and Technology, 54, 060201.

Vaezi, M., & Chua, C. K. (2011). Effects of layer thickness and binder saturation level parameters on 3D printing process. The International Journal of Advanced Manufacturing Technology, 53(1), 275-284.

Walters, P., Huson, D., Parraman, C., & Stanić, M. (2009). 3D printing in colour: technical evaluation and creative applications.

Wimpenny, D., Ian, Banerjee, S., & University, D. M. (2008). Electrostatic printing method and its use in rapid prototyping: WO Patent WO/2008/096,105.

Wimpenny, D. I., Banerjee, S., & Jones, J. (2008, 2009). Laser printed elastomeric parts and their properties.

Wyszecki, G., & Stiles, W. S. (1967). Color science: Wiley New York.